Accepted Manuscript

Membrane lipid modifications and therapeutic effects mediated by hydroxydocosahexaenoic acid on Alzheimer's disease

Manuel Torres, Samantha L. Price, Maria A. Fiol-deRoque, Amaia Marcilla-Etxenike, Hasna Ahyayauch, Gwendolyn Barceló-Coblijn, Silvia Terés, Loukia Katsouri, Margarita Ordinas, David J. López, Maitane Ibarguren, Félix M. Goñi, Xavier Busquets, Javier Vitorica, Magdalena Sastre, Pablo V. Escribá

Please cite this article as: Manuel Torres, Samantha L. Price, Maria A. Fiol-deRoque, Amaia Marcilla-Etxenike, Hasna Ahyayauch, Gwendolyn Barceló-Coblijn, Silvia Terés, Loukia Katsouri, Margarita Ordinas, David J. López, Maitane Ibarguren, Félix M. Goñi, Xavier Busquets, Javier Vitorica, Magdalena Sastre, Pablo V. Escribá. Membrane lipid modifications and therapeutic effects mediated by hydroxydocosahexaenoic acid on Alzheimer's disease. *BBA - Biomembranes* (2014), doi: 10.1016/j.bbamem.2013.12.016

Membrane lipid modifications and therapeutic effects mediated by hydroxydocosahexaenoic acid on Alzheimer's disease

Manuel Torres[a, *], Samantha L. Price[b], Maria A. Fiol-deRoque[a], Amaia Marcilla-Etxenike[a], Hasna Ahyayauch[c], Gwendolyn Barceló-Coblijn[a], Silvia Terés[a], Loukia Katsouri[b], Margarita Ordinas[a], David J. López[a], Maitane Ibarguren[a], Félix M. Goñi[c], Xavier Busquets[a], Javier Vitorica[d], Magdalena Sastre[b, *], Pablo V. Escribá[a, *]

[a] Laboratory of Molecular Cell Biomedicine, University of the Balearic Islands, Palma de Mallorca, Spain

[b] Division of Brain Sciences, Imperial College London, London, United Kingdom

[c] Biophysics Unit (CSIC, UPV/EHU) and Department of Biochemistry and Molecular Biology, University of the Basque Country, Bilbao, Spain

[d] IBIS Seville Biomedical Research Institute, Virgen del Rocio University Hospital, CSIC — University of Seville, and CIBERNED, Seville, Spain

*To whom correspondence should be addressed:

Laboratory of Molecular Cell Biomedicine, Department of Biology, University of the Balearic Islands, Crta. Valldemossa km. 7.5, 07122 Palma de Mallorca, Spain. Tel.: + 34 97117 3331; fax: + 34 97117 3184.

Division of Brain Sciences, Imperial College London, Hammersmith Hospital, Du Cane Road, W12 0NN London, United Kingdom. Tel.: +44 2075946673; fax: +44 2075946548.

E-mail addresses: manuel.torres.phd@gmail.com (M. Torres), m.sastre@imperial.ac.uk (M. Sastre), pablo.escriba@uib.es (P.V. Escribá).

Abstract

Alzheimer's disease (AD) is a neurodegenerative pathology with relevant unmet therapeutic needs. Both natural aging and AD have been associated with a significant decline in the omega-3 polyunsaturated fatty acid docosahexaenoic acid (DHA), and accordingly, administration of DHA has been proposed as a possible treatment for this pathology. However, recent clinical trials in mild-to-moderately affected patients have been inconclusive regarding the real efficacy of DHA in halting this disease. Here, we show that the novel hydroxyl-derivative of DHA (2-hydroxydocosahexaenoic acid — OHDHA) has a strong therapeutic potential to treat AD. We demonstrate that OHDHA administration increases DHA levels in the brain of a transgenic mouse model of AD (5xFAD), as well as those of phosphatidylethanolamine (PE) species that carry long polyunsaturated fatty acids (PUFAs). In 5xFAD mice, administration of OHDHA induced lipid modifications that were paralleled with a reduction in amyloid-β (Aβ) accumulation and full recovery of cognitive scores. OHDHA administration also reduced Aβ levels in cellular models of AD, in association with alterations in the subcellular distribution of secretases and reduced Aβ-induced tau protein phosphorylation as well. Furthermore, OHDHA enhanced the survival of neuron-like differentiated cells exposed to different insults, such as oligomeric Aβ and NMDA-mediated neurotoxicity. These results were supported by model membrane studies in which incorporation of OHDHA into lipid-raft-like vesicles was shown to reduce the binding affinity of oligomeric and fibrillar Aβ to membranes. Finally, the OHDHA concentrations used here did not produce relevant toxicity in zebrafish embryos in vivo. In conclusion, we demonstrate the pleitropic effects of OHDHA that might prove beneficial to treat AD, which suggests that an upstream event, probably the modulation of the membrane lipid composition and structure, influences cellular homeostasis reversing the neurodegenerative process. This Article is Part of a Special Issue Entitled: Membrane Structure and Function: Relevance in the Cell's Physiology, Pathology and Therapy.

Keywords

1. Introduction

Alzheimer's disease is a neurodegenerative disorder that produces severe cognitive impairment as it progresses. This pathology is the main neurological cause of dementia and it is suffered by 36 million people worldwide, elderly adults in most cases (World Alzheimer Report 2011). Unfortunately, there are still no effective treatments that mitigate the neurological deficits associated with AD. Currently, these patients may be treated with two classes of approved drugs that ameliorate the symptoms of AD, acetylcholinesterase inhibitors and NMDA receptor antagonists, although their clinical efficacy is considered to be very limited [1]. Other promising therapeutic approaches have been proposed for AD, such as statins and non-steroidal anti-inflammatory drugs, although they have yet to offer conclusive results in clinical trials [2], [3], [4].

DHA (22:6 n-3) is the most abundant omega-3 PUFA in the brain and it is tightly involved in the functioning of the central nervous system (CNS) [5], particularly in neurogenesis, synaptogenesis and synaptic transmission [6], [7]. This fatty acid is obtained through the diet and its deficiency is associated with age-related cognitive decline and with neurodegenerative diseases, such as AD [8], [9]. In recent years, PUFAs like DHA have gained much attention due to promising results that suggest they may be useful to treat AD. In this sense, several studies have demonstrated that oral intake of DHA or fish oil reduces AD-associated brain pathology, for instance, improving cognitive deficits, protecting against synaptic degeneration and lowering Aβ levels in transgenic AD mouse models [10], [11], [12], [13]. Moreover, these results are supported by epidemiological studies indicating an inverse relationship between DHA intake and AD incidence, which correlate high DHA levels with reduced risk of cognitive dysfunction [14], [15]. However, direct administration of DHA in clinical trials only showed improved cognition of a small subgroup of patients with very mild cognitive dysfunction and there was no clear effect in most patients [16], [17], even though DHA administration improves the physiological, but not pathological, age-related cognitive decline [18].

In this context, there would appear to be a link between AD and lipid alterations in neuronal membranes, especially diminished DHA levels. Therefore, molecules that are effective in restoring DHA and normalizing the membrane lipid composition could constitute therapeutic tools to treat AD. In the present work, we show that OHDHA regulates membrane lipid composition and structure, cell signaling and, additionally, it improves cognitive scores in animal models of AD [19], thereby representing a novel therapeutic candidate for the treatment of AD. This DHA derivative bears a hydroxyl group on the α-carbon that impedes its β-oxidation and increases its half-life in lipid membranes. Interestingly, natural DHA hydroxyl derivates are also produced in the brain, such as neuroprotectin D1 (NPD1), and like DHA, NPD1 is also strongly diminished in the brain of AD patients [20]. The biological function of this molecule has been related to multiple neuroprotective effects, such as antioxidant, anti-inflammatory and anti-apoptotic roles. NPD1 also downregulates Aβ peptide production by modulating β- and α-secretase activities, and it favors neuronal survival against Aβ toxicity [20], [21]. In the present work we found that OHDHA administration leads to enrichment of membranes in long PUFAs, which is associated with neuronal survival and neuroregeneration, so that OHDHA mimics the effects of NPD1. These changes in membrane lipid composition could facilitate the maintenance of a functional cell membrane structure that, in the case of AD, may reverse neurons from a pathological to a healthy condition [22]. Specifically, we show that by downregulating Aβ generation and Aβ-induced tau protein hyperphosphorylation, OHDHA promotes neuroprotection, and cell survival against different known AD-associated insults. In addition, this compound can also induce neuron stem cell proliferation via molecular and cellular mechanisms that remain largely unknown [19] and patients. Thus, OHDHA-induced neuron survival and proliferation should lead to improved cognition in AD models [19] and patients. In conclusion, OHDHA is presented here as a novel therapeutic candidate for the treatment of the AD-related neurodegeneration.

2. Material and methods

2.1. Transgenic mice and treatments

A double transgenic PS1/APP mouse model was used in this work (5xFAD; line Tg6799) that harbors five human mutations associated to familial AD: the *Swedish* (K670N/M671L), *Florida* (I716V) and *London* (V717I) mutations in APP (amyloid precursor protein); and a human mutated PS1 (presenilin 1) harboring the M146L and L286V clinical mutations. Both these transgenes are expressed under control of the Thy-1 promoter. These mice display cognitive decline from 4 months of age [23]. These transgenic 5xFAD and wild type (WT) mice were purchased from Jackson Laboratories (USA), and they were maintained on a B6/SJL hybrid genetic background (C57BL/6 x SJL) by crossing heterozygous transgenic mice with B6/SJL WT (F1) breeders. All animals were housed at a controlled temperature and

humidity (22 ± 2 °C; 70% humidity) on a 12 h–12 h light–dark cycle, and they were provided a standard laboratory diet ad libitum (Panlab A03; Barcelona, Spain).

WT and transgenic 5xFAD male mice were orally administered OHDHA (Lipopharma Therapeutics; Palma de Mallorca, Spain) dissolved in 5% ethanol at a dose of 15 mg/kg·day or the vehicle solution alone (5% ethanol; 15 ml/kg·day). These treatments started when the mice reached 3 months of age (dosed 5 days/week) and they were continued until the mice reached 7 months of age. During the last month of treatment, all the animals were submitted to a hypocaloric diet necessary to perform the selected behavioral spatial learning and memory test (food craving test in a radial arm maze) [24]. The results concerning the radial arm maze test have been reported previously [19], and a summary table (containing more relevant findings and total number of animals that were used for the test) has been also included in the discussion section of the present work (Table 4). Following the behavioral test, the mice were kept on normal diet (and treatment) for an additional week, after which they were euthanized, and their brain was removed immediately and dissected down the midline on a cold surface. Having removed the cerebellum, each cerebellum-free hemibrain was frozen in liquid nitrogen and stored at − 80 °C. A total number of 9 animals were used in this work: 3 vehicle-treated WT, 3 vehicle-treated 5xFAD and 3 OHDHA-treated 5xFAD mice. All the protocols employed were approved by the Bioethical Committee of the University of the Balearic Islands, and they are in agreement with national and international regulations on animal welfare.

2.2. Lipid extraction and determination of cholesterol content

One hemi-brain from each animal was homogenized in a guanidine-salt buffer (RLT Buffer; Qiagen) at 1:20 (w:v) using a blade homogenizer (Polytron PT3100). The samples were then incubated at room temperature for 10 min and centrifuged for 5 min (10,000 g, 4 °C). The resulting supernatant was recovered, aliquoted and stored at − 80 °C. Lipids were extracted using Bligh and Dyer's method [25]. The recovered organic phase was stored under a N_2 atmosphere at − 80 °C. The cholesterol (Cho) content was determined as described previously [26]. Briefly, lipid extracts were evaporated under argon flow for at least 2 h and then resuspended in isopropanol. Total cho was measured in an aliquot (10 μl) using an enzymatic colorimetric kit (Biosystems; Barcelona, Spain) and determined through the appearance of a product absorbing at 500 nm.

2.3. Sphingolipid and phospholipid lipidomic analysis

Lipidomic studies were performed as described previously [27], [28]. Liquid cromatography/mass spectrometry (LC/MS) analysis was performed on a Waters Aquity UPLC system connected to a Waters LCT Premier orthogonal accelerated time of flight mass spectrometer (Waters), operated in positive electrospray ionization mode. Full scan spectra from 50 to 1500 Da were acquired and individual spectra were summed to provide data points each 0.2 s. Mass accuracy and reproducibility were maintained by using an independent reference spray via LockSpray interference. The analytical column was a 100×2.1 mm inner diameter, 1.7 μm C8 Acquity UPLC bridged ethylene hybrid (Waters), thermostated at 30 °C. The two mobile phases both contained 5 mM ammonium formate: phase A, MeOH/H_2O/HCOOH (74:25:1, v/v); and phase B: MeOH/HCOOH (99:1, v/v). Quantification was carried out on 50 mDa windows using the extracted ion chromatogram of each compound, and the linear dynamic range was determined by injecting standard mixtures. Positive identification of compounds was based on accurate mass measurement, with an error of < 5 ppm, and LC retention times compared to that of standards (± 2%).

For lysosphingolipid quantification, extracts were analyzed by LC/MS/MS with a system consisting of a Waters Alliance 2690 LC pump equipped with an autosampler and connected to a Quattro LC triple-quadrupole mass spectrometer (Micromass, Manchester, UK). Separation was achieved on a Purospher STAR-RP-18 column (125×2 mm, 5 μm; Merck) using the same mobile phases as described above with a flow rate of 0.3 ml min^{-1}. The gradient used was: 0.0 min, 50% B; 2 min, 50% B; 7 min, 100% B; 17 min, 100% B; 19 min, 50% B; and 26 min, 50% B. MS/MS detection was performed with an electrospray interface operating in the positive ion mode acquiring the following selected reaction monitoring transitions: C17 d-*erythro*-dihydrosphingosine-1-phosphate, 368–252 Da, collision energy 18 eV; and S1P, 380–264 Da, collision energy 16 eV.

2.4. Cell culture and treatments

2.4.1. Cell lines

Mouse neuroblastoma N2a cells stably transfected with human *Swedish*-mutated APP, also called N2aSw (kindly provided by Gopal Thinakaran; University of Chicago, USA), were maintained in a 1:1 (v:v)

mixture of Dulbecco's Modified Eagle Medium (DMEM) and OPTI-MEM (Invitrogen) supplemented with 5% fetal bovine serum (FBS; Sigma), penicillin/streptomycin (PAA) and G-418 (final concentration, 0.2 mg/ml). N2aSw cells were transfected with PS1-GFP (kindly provided by Dr Christoph Kaether; Leibniz Institute for Age Research; Germany) or BACE1 (kindly provided by Jochen Walter; University of Bonn; Germany) cDNAs using the calcium phosphate method [29].

Human neuroblastoma SH-SY5Y cells were maintained in DMEM Hams F12 (Invitrogen) supplemented with 10% FBS (Sigma), penicillin/streptomycin (PAA), non-essential aminoacids (Sigma) and 2 mM L-glutamine (Sigma). Differentiation of these cells to a neuron-like phenotype was carried out as described previously [30]. Briefly, cells were plated in poly-L-Lysine pre-coated dishes and 24 h later, the medium was replaced with fresh medium supplemented with 10 μM retinoic acid (Sigma). The cells were then incubated in the dark for 5 days and the medium was replaced with medium without serum and supplemented with 50 ng/ml of human brain-derived neurotrophic factor (hBDNF; Alomone Labs; Tel Aviv, Israel). Finally, the cells were incubated for 6 days to complete differentiation.

Embryonal multipotent stem P19 cells were cultured in α-Minimum Essential Medium (αMEM; Sigma) containing 10% FBS (Sigma) and penicillin/streptomycin (PAA). Differentiation of P19 cells to a neuron-like phenotype was carried out as described previously [31]. Briefly, differentiation was induced by 300 nM retinoic acid for 48 h, followed by sub-culturing 1:4 in the presence of 300 nM retinoic acid for another 48 h. Incubation with retinoic acid was performed in the dark. Cell clusters were then seeded 1:4 in 6-well plates for an additional 24 h to complete the differentiation process.

MDCK cells, stably expressing the human APP-GFP fusion protein were cultured in DMEM supplemented with 5% FBS (Sigma) and penicillin/streptomycin (PAA). All cell lines were incubated in a 5% CO_2 atmosphere at 37 °C.

2.4.2. Hydroxylated lipids, Aβ and NMDA treatments.

Stock solutions containing 100 mM OHDHA in DMSO were used for cell treatments. DMSO was diluted to be below 0.1% in the medium. N2aSw cells were incubated in the presence or absence of 5, 10 or 50 μM OHDHA for 24 h. Neuron-like differentiated SH-SY5Y cells were exposed to oligomeric Aβ (5 μM) for 24 h in the presence or absence of OHDHA (5 and 10 μM). Neuron-like differentiated P19 cells were treated for 24 h with OHDHA (10 μM), and then for 30 min with NMDA (10 mM, Sigma) in fresh media containing glycine (530 μM, Sigma) and calcium (10 mM, Sigma). Finally, APP-GFP MDCK cells were treated for 72 h with OHDHA at 1, 3, 10, 15, 20, 25, 30, 40, 50, 60 and 70 μM.

2.5. Protein isolation and Western blotting

Hemibrains from WT and 5xFAD mice were homogenized in a guanidine-thiocyanate-based buffer (RLT buffer, Qiagen) as described above (Section 2.2) and the protein was isolated using the All Prep DNA/RNA/protein isolation kit (Qiagen) following the manufacturer's instructions. The protein pellet was resuspended in Laemmli's SDS-PAGE loading buffer and incubated overnight at room temperature prior to use. Alternatively, the protein was extracted from SH-SY5Y cells as described previously [32]. In the case of N2aSw cells, soluble αAPP and Aβ peptide levels were determined in harvested cell media [33]. The Aβ peptide was immunoprecipitated from the medium overnight at 4 °C using the 2964 antibody [34] and Protein-A sepharose beads (Invitrogen). The beads were then recovered by centrifugation (500 g, 5 min, 4 °C), washed three times and diluted in Laemmli's buffer.

Protein samples (5–20 μg) were resolved on 16% (for brain samples) or 4–12% (for cell culture samples) polyacrylamide gels, using Tris-tricine or Tris-glycine electrophoresis buffer. The proteins were then transferred to nitrocellulose membranes (GE, Amersharm) that were subsequently blocked with 5% (w:v) non-fat dry milk in 0.1% (v:v) Tween-20 PBS. These membranes were then probed overnight at 4 °C with the corresponding primary antibody: anti-Aβ1-16 (clone 6E10, 1:4000; Signet Labs.), anti-Ser202/Thr205-PHF-tau (clone AT8, 1:1000; Pierce), anti-phospho-Ser202-tau (clone CP13; 1:1000; kindly provided by Dr. Peter Davies, Albert Einstein College of Medicine, USA), anti-total-tau (Tau46; 1:2000; Pierce), anti-α-tubulin (1:5000; Sigma). Antibody binding was detected with the IRDye-800CW-labeled anti-mouse IgG for brain samples (1:5000; LI-COR Inc.) or horseradish peroxidase-conjugated anti-mouse IgG for cell samples (1:2000; GE Healthcare). Membrane fluorescence was detected using an Odyssey Infrared Imaging System (LI-COR Inc.) and membrane chemiluminescence was detected by ECL (GE, Amersham) in an automated SRX 101A developer (Konica). The intensity of the bands was quantified by densitometry using the Image J software (National Institutes of Health) and normalized to α-tubulin.

2.6. RNA isolation, reverse transcription and real time RT-PCR

RNA isolation, reverse transcription (RT) and quantitative real-time PCR were performed according to the Minimum Information for publication of Quantitative real-time PCR Experiments (MIQE) guidelines [35]. After homogenization in RLT-buffer (see Section 2.2), total RNA was isolated from the brain using the All Prep DNA/RNA/protein isolation kit (Qiagen) according to the manufacturer's instructions. Residual DNA was removed by incubation with DNase (Qiagen) prior to performing reverse transcription. RT was performed with the High Capacity cDNA Archive kit (Applied Biosystems) on 4 µg of the total RNA template, following the manufacturer's recommendations [36].
Human and mouse APP gene products were amplified from 5xFAD brain cDNA samples using specific primers: human/mouse APP695 forward (5′-CATCATGGTGTGGTGGAG-3′), human APP695 reverse (5′-GCGATAATGAGTAAATCATAAAAC-3′) and mouse APP695 reverse (5′-GGGTGAGTAAATAAACGGAA-3′). For each assay, a standard curve was first defined using increasing amounts of cDNA and in all cases, the slope of these curves indicated the optimal amplification efficiency (slope 3.2-3.4). GAPDH was used as a control housekeeping gene and this amplification was detected by using commercial Taqman probes (Mm99999915_g1; Applied Biosystems) according to the manufacturer's instructions. GAPDH was amplified in parallel with the target gene. The results were expressed using the comparative Ct method, as described elsewhere [36], [37]. As a control condition, we selected mouse APP expression in WT mice. In consequence, the expression of both mouse and human APP genes, for all mouse strains and treatments, was referenced to mouse APP expression levels observed in WT mice.

2.7. Immunocytochemistry

Mouse neuroblastoma N2aSw cells were fixed and permeabilized in 100% methanol at − 20 °C for 20 min, the cells were then rehydrated in PBS for 10 min and blocked in 1% BSA in PBS for 20 min at room temperature. Subsequently, the cells were incubated with the primary antibody diluted in 1% BSA in PBS overnight: mouse anti-APP (clone 6E10, 1:200; Signet Labs.), rabbit anti-BACE-1 (1:50; Cell Signaling), rabbit anti-APP-C-terminal (R1(57); kindly provided by Dr P. Mehta, New York State Institute for Basic Research in Developmental Disabilities, USA); mouse anti-Lamp-1 (1:200; Abcam) and/or rabbit anti-LC3 (1:200; Abcam). The cells were then washed 3 times with PBS, and incubated with Alexa 488 and 594-conjugated secondary antibodies (Invitrogen) at room temperature in the dark. After 3 washes with PBS, the coverslips were mounted onto slides using Vectashield mounting solution containing DAPI (Vector Labs) and images were captured on a Leica LAS AF SP5 confocal microscope. N2aSw cells transfected with PS1-GFP were also permeabilized, rehydrated and analyzed as above. MDCK cells expressing APP-GFP were fixed with 4% paraformaldehyde (Sigma) for 30 min and mounted onto slides using Vectashield mounting solution (Vector Labs). Images were captured by confocal microscopy (Becton Dickinson) and the number of fluorescent APP-containing vesicles per cell was calculated with AttoVision software (Becton Dickinson).

2.8. Amyloid-β42 peptide preparation

Monomeric, oligomeric and fibrillar Aβ were prepared as described previously [38]. An Aβ42 stock solution was prepared by dissolving the peptide at 1 mg/ml in hexafluoro-2-propanol (HFIP; Sigma) to render the Aβ monomeric. HFIP was removed under vacuum in a SpeedVac (Millipore) and the peptide film was stored desiccated at − 20 °C. For the Aβ42 monomer preparation, the peptide film was resuspended in DMSO just prior to use at a concentration of 5 mM and it was sonicated for 10 min in a bath-type ultrasound device. Oligomeric Aβ was generated by diluting the monomeric preparation to 100 µM in 150 mM NaCl, 1 mM EDTA, 10 mM Tris–HCl [pH 7.4], which was incubated for 24 h at 4 °C. Finally, fibrillar Aβ was generated by adding 10 mM HCl to the initial solution of monomeric Aβ to obtain 100 µM Aβ [pH 2.0], and this solution was then incubated for 48 h at 37 °C.

2.9. Aβ binding assays to lipid vesicles

2.9.1. Preparation of lipid vesicles

Large unilamellar vesicles (LUVs) were generated as described previously [39]. LUVs composed of sphingomyelin (SM) and Cho (1:1 mol ratio) or SM:Cho:OHDHA (1:1:0.1 mol ratio) were extruded in 10 mM Hepes, 1 mM EDTA, 100 mM NaCl [pH 7.4] using an extruder with 200 nm filters. The lipid composition of LUVs was quantified as described previously [40], showing that the final composition did not differ significantly from the initial lipid mixture.

2.9.2. Isothermal Titration Calorimetry (ITC)

ITC measurements were performed in a VP-ITC Micro-calorimeter (MicroCal, Inc., Northampton, USA) as described previously [41], [42]. Briefly, the experiments were set-up with 23 μM of Aβ peptide (monomer, oligomer or fibrils) in the cell at 37 °C (cell volume: 1.4 ml) and 35 mM of LUV in the syringe. Thirty injections of 10 μl were administered at an interval between injections of 10 min. All the thermodynamic parameters were calculated using MicroCal Origin software. The binding constant Ka (Kd = 1 / Ka) and enthalpy (ΔH) were obtained from the fitting of ITC isotherms, and the Gibbs free energy (ΔG) and entropy (ΔS) of binding were determined from the expression:

$$\Delta G = \Delta H - T\Delta S = -RTlnKa$$

where R is the gas constant and T is temperature.

2.10. Cell viability (MTT)

Cell viability was determined using the MTT (methyl-thiazolyl diphenyl tetrazolium bromide) method, as described previously [32]. The MTT reagent (Sigma) was diluted to a final concentration of 0.5 mg/ml in PBS and added to the cell culture for 2 h. Mitochondrial dehydrogenases in viable cells reduced the tetrazolium salt, yielding water insoluble colored formazan crystals. The MTT reagent was then removed and the formazan crystals solubilized by adding one volume of DMSO for 5 min, and after gentle shaking, the absorbance of the solution was determined at 570 nm.

2.11. Zebrafish embryo toxicity

Evaluation of OHDHA toxicity in zebrafish embryos was performed as described previously [43] and following the OECD (Organization for Economic Co-operation and Development) Draft Guidelines. Briefly, five concentrations of OHDHA were added to different tanks of water: 1, 3, 10, 30 and 100 mg/l. The OHDHA was primarily dissolved in DMSO to obtain the working stocks, keeping the final concentration of DMSO always below 0.1% in the toxicity assays. Each concentration of OHDHA was tested in 20 individual embryos for 24, 48 and 72 h at 25 °C. After incubation, the percentage of embryos showing embryo mortality, sub-lethal effects, teratogenic effects and viability was determined.

2.12. Statistical analysis

Data were expressed as the mean ± SEM. Comparison between two groups of data was performed using a two-tailed *t*-test. For comparison between several groups, we used one-way ANOVA followed by Tukey's *post hoc* multiple comparisons (Statgraphics plus 3.1). The level of significance was set at 95% of confidence ($p < 0.05$).

3. Results

3.1. Effects of OHDHA on membrane lipid composition in the brains of 5xFAD mice

The membrane lipid species in the brains of WT, 5xFAD and OHDHA-treated 5xFAD mice were analyzed by lipidomic analysis (Fig. 1, Table 1 and Fig. S1). The most abundant lipid species detected were the different classes of PE (see Fig. S1), with all PE species together constituting approximately half of the total membrane lipids in the brain of WT mice (47.77 ± 4.26%). A significant increase in total PE levels in the brain of 5xFAD mice was observed after treatment with OHDHA (47.26 ± 6.11% increase with respect to untreated 5xFAD mice), and these OHDHA-treated mice also showed higher PE levels compared to WT mice (43.80 ± 5.96%; Fig. 1A). In addition, the elevated PE levels in the brain of OHDHA-treated mice were due to a general increase in all analyzed PE species (Fig. S1).

Treatment with OHDHA also increased the concentration of PUFA-containing phospholipids (containing 5 or more double bonds, e.g. DHA or EPA-containing phospholipids) compared to WT and 5xFAD untreated mice, whereas it had a smaller impact on saturated fatty acid-containing phospholipids (Figs. 1B and C). The higher level of PUFA -containing phospholipids in the brain of 5xFAD mice was mainly due to the increase in PE species provoked by OHDHA (see Table 1). In this sense, the most important increase among diacyl-PE subspecies was observed in PE 40:6 (an 85.2 ± 8.7% increase with respect to the WT), while other polyunsaturated diacyl-PE subspecies also showed important elevations in the brain of 5xFAD mice after OHDHA treatment (40:5, 38:5, 38:4, 36:5 and 36:4; Table 1). This result is compatible with the elevated levels of DHA in lipid membranes after OHDHA treatment since diacyl-PE 40:6 may be constituted principally by 22:6 (DHA) and 18:0 fatty acids. Indeed, our lipidomic analysis

7

also revealed that lyso-PE 18:0 is the most abundant subspecie among all the lyso-PE lipids (not shown), such that the diacyl-PE 40:6 detected must carry DHA at position C2 of glycerol.

In the same context, an analysis of the hydrocarbon chain length of Table 1-showed diacyl-PE subspecies revealed that long (40C) and medium (36–38C)-chain-fatty acid-containing PEs increased more strongly in the brain of 5xFAD mice after OHDHA treatment than short-chain (32–34C) fatty-acid-containing PEs (a $50.59 \pm 8.04\%$ and $40.47 \pm 7.04\%$ increase, respectively, compared to the WT). Again, no significant differences were observed when comparing WT and 5xFAD control mice (Table 1). All these data demonstrate that OHDHA produces an elevation in the PE phospholipids in the brain of 5xFAD mice that preferentially contain long/middle polyunsaturated acyl chains (40:6, 40:5, 38:5, 38:4, 36:5 and 36:4). Finally, a significant increase in the levels of phosphatidylinositol (PI) in the brain of 5xFAD mice was also associated with OHDHA treatment (Fig. 1E). By contrast, no significant changes were observed in other phospholipid species, such as phosphatidylcholine (PC) or phosphatidylserine (PS: Figs. 1D and F), nor were there significant differences in other lipid classes, such as cholesterol, sphingolipids (sphingomyelin and dihydrosphingomyelin) and ceramides (ceramide, hexosyl-ceramides and lactosyl-ceramide) (Figs. 1G, H and I, respectively). However, the higher levels of PE in the brain of OHDHA-treated mice induced modest general decreases in other lipids, such as Cho, diacyl-PC and SM (see Fig. S1). In conclusion, changes in lipid membrane composition induced by OHDHA may influence the lipid membrane structure, provoking the formation of liquid disordered prone structures [44].

3.2. OHDHA treatments induce a reduction in Aβ levels and tau protein phosphorylation in transgenic 5xFAD mice and cellular models of AD

The production and accumulation of Aβ is one of the most studied neuropathological features of AD. The accumulation of Aβ correlates strongly with synaptic degeneration, and with memory and learning deficits in the 5xFAD model [23], [45], [46]. Indeed, serious cognitive deficits were reported previously in these mice when cognitive impairment was analyzed using the radial arm maze test, as reflected by the increase in the time spent in completing the test and the number of errors compared to WT mice [19]. On the other hand, enzymes implicated in the amyloidogenic route (β- and γ-secretases) are both integral membrane proteins that are highly regulated by the membrane lipid environment [47], [48]. In this context, we hypothesized that OHDHA-mediated membrane lipid modifications might influence Aβ generation/accumulation in the brain of 5xFAD mice. Thus, we investigated the effect of OHDHA on Aβ production in 5xFAD brain samples. As expected, we only identified monomeric Aβ peptide in 5xFAD brain samples (Fig. 2A, upper panel), in which there was a modest, yet significant downregulation of Aβ levels following OHDHA treatment (Fig. 2A, middle panel). In addition, human APP transgene expression remained unmodified by OHDHA in these samples (see Fig. S2), demonstrating that Aβ levels are not affected by changes in human APP gene expression. In parallel with the reductions in Aβ, OHDHA-treated 5xFAD mice also displayed a significant recovery of learning and memory capabilities compared to the 5xFAD control mice, evident through the reduction in the time spent and working/reference memory errors committed when completing the behavioral test (previously reported by [19], see discussion below). Thus, these results suggest that the modifications of lipids in brain membranes are associated with a decrease in Aβ levels and improved cognitive scores in this AD model.

The effect of DHA (and probably OHDHA) on Aβ production is strongly influenced by dietary lipid intake. Indeed, this effect might be underestimated due to the presence of specific lipids in the diet that stimulate amyloidogenesis [49]. Therefore, we further studied this issue in a cellular model of neuroblastoma cells stably expressing the *Swedish*-mutant form of APP (N2aSw). In this context, the Aβ produced and secreted into the cell culture medium was immunoprecipitated and analyzed by immunoblotting. Cell cultures were treated with 5 and 10 μM of OHDHA, which led to a drastic reduction in Aβ in the medium over 24 h (Fig. 2B). We also determined the soluble APPα (sAPPα) levels in the culture medium (Fig. 2B) and the full length APP (flAPP) in cell extracts (not shown) using the 6E10 antibody. Unlike previous reports [12], we found no remarkable changes in either sAPPα or flAPP, suggesting that the non-amyloidogenic route is apparently unaffected by OHDHA and that the changes observed in Aβ are not due to the downregulation of human APP expression. These data confirmed our previous results in the brain of OHDHA-treated 5xFAD mice.

On the other hand, tau phosphorylation was tested in the brain of 5xFAD mice at Ser202/Thr205 (AT8 epitope) and Ser202 (CP13 epitope). Interestingly, AT8 antibody retrieved none or very low signal when using these brain samples (not shown). However, when using CP13 antibody our experiments showed a clear band of ca. 64 kDa, especially in 5xFAD mice (Fig. 2A, upper panel). Indeed, tau phosphorylation

in 5xFAD brain samples was statistically increased compared to WT controls, whereas this increase was prevented in OHDHA-treated 5xFAD mice (Fig. 2A, lower panel). Furthermore, total tau levels were determined with Tau46 antibody in these samples. Labeling with this antibody showed several specific bands ranging from 49 to 73 kDa (probably corresponding to different phosphorylated forms of tau protein) (Fig. 2A, upper panel). Minimal differences in total tau were found and, consequently, phospho/total tau ratio showed similar differences among WT, 5xFAD and OHDHA-treated 5xFAD mice to those shown by phospho-Ser202-tau (Fig. 2A, lower panel). We also tested the efficacy of OHDHA in reducing the Aβ-mediated hyperphosphorylation of tau in a cellular model of neuron-like differentiation of SH-SY5Y cells [30]. For these assays, differentiated neuron-like cells were stimulated for 24 h with oligomeric Aβ (5 μM) to induce tau hyperphosphorylation in the presence or absence of OHDHA (5 and 10 μM). The addition of Aβ strongly induced tau phosphorylation at Ser202/Thr205 (AT8 epitope), although the presence of OHDHA markedly and significantly reduced the effect of Aβ on tau phosphorylation, which was similar to that found in unstimulated controls (Fig. 2C). Consequently, OHDHA appears to inhibit Aβ-induced tau hyperphosphorylation.

Although there is strong evidence that membrane lipids participate in the amyloidogenic pathway, the mechanism by which DHA or OHDHA regulates Aβ generation still remains largely unknown. To determine whether OHDHA affects the levels and distribution of flAPP, as well as the secretases responsible for amyloidogenic APP cleavage, we evaluated the subcellular localization of APP, PS1 (the protein containing the catalytic site of γ-secretase complex [50]) and BACE-1 (the principal β-secretase enzyme in the brain [51]) in N2aSw cells. In these assays, N2aSw cells were treated with OHDHA (10 μM) for 24 h, and the subcellular distribution of APP and BACE-1 was analyzed by immunofluorescence with the 6E10 and anti-BACE1 antibodies, respectively (Fig. 3, panels A1 and A2 or A5 and A6, respectively). The distribution of PS1 was visualized in N2aSw cells transfected with PS1-GFP cDNA (Fig. 3, panels A3 and A4). A diffuse distribution of APP, PS1 and BACE was observed in the cytoplasm and Golgi apparatus of N2aSw control cells (exposed to the DMSO vehicle alone: Fig. 3, panels A1, A3 and A5, respectively). Following exposure to OHDHA these proteins localized to defined vesicle-like punctae (Fig. 3, panels A2, A4 and A6, respectively), suggesting that OHDHA provokes the clustering of APP, PS1 and BACE-1 into defined cell vesicles/organelles. These results indicate that the recruitment of these proteins into cell vesicles actively participates in the OHDHA-mediated inhibition of amyloidogenesis (Fig. 2B). In order to elucidate the possible implication of the endolysosomal system on APP/PS1/BACE-1 vesicle recruitment and Aβ level downregulation in OHDHA-treated N2aSw cells, we further studied the nature of these vesicles by confocal immunofluorescence co-localization of APP and LC3 (autophagic vesicle marker), or APP and Lamp1 (lysosome marker). Our results clearly showed no co-localization between APP and LC3, whereas APP and Lamp1 showed some weak co-localization in OHDHA-treated cells (Fig. S3), suggesting that the origin of these APP-positive vesicles is not the autophagic or lysosomal system. On the other hand, these results were confirmed in MDCK cells stably expressing the APP-GFP fusion protein, where the clustering of APP alone was shown to be induced by OHDHA over a wider range of concentrations (Fig. 3B, testing exposure to 1, 3, 10, 15, 20, 25 and 30 μM OHDHA for 72 h). These results confirmed the effect previously observed in N2aSw cells, as APP clustering in vesicles first appeared in the presence of 10 μM OHDHA, and it was more prominent at 15, 20 and 25 μM (Fig. 3, panels B1, B2, B3 and B4, respectively). Thus, GFP-positive vesicles rapidly accumulated and this effect became saturated between 20 and 30 μM, indicating a reduced amyloidogenic secretase activity in OHDHA-treated MDCK cells. Indeed, quantifying the fluorescent vesicles allowed the half maximal effective concentration (EC_{50}) to be determined as 17.8 μM under these experimental conditions (Fig. 3, panel B5).

3.3. Neuroprotective effect of OHDHA on neuron-like differentiated cells exposed to an Aβ or a NMDA-mediated toxic insult

Our results demonstrate that OHDHA regulates the lipid composition of membranes, as well as Aβ accumulation and tau phosphorylation in the brain of 5xFAD mice, suggesting a possible neuroprotective role for OHDHA. Therefore, we studied whether OHDHA might promote neuron survival by examining the response of human neuroblastoma SH-SY5Y cells and embryonic stem P19 cells differentiated to a neuron-like phenotype when confronted by known neurotoxic compounds. First, neuron-like cells differentiated from SH-SY5Y cells were incubated with oligomeric Aβ for 24 h [52], in the presence or absence of OHDHA, and cell viability was determined with the MTT assay. Exposure to Aβ42 reduced cell viability by 20.48 ± 1.18% and while neuronal death caused by Aβ was inhibited in the presence of 5 μM OHDHA, in the presence of 10 μM OHDHA the number of neuron-like cells was even greater than

that of the control cells not exposed to Aβ (37.85 ± 1.55% over untreated control cells: Fig. 4A). Similarly, NMDA-induced Ca^{2+} excitotoxicity caused a reduction in the number of P19-derived cells (a 39.42 ± 6.24% loss compared to untreated control cells: Fig. 4B). In this context, exposure to OHDHA (10 μM, 24 h) induced an increase in the number of viable cells with respect to NMDA-treated and untreated control cells (133.58 ± 32.26% and 94.36 ± 32.26%, respectively: Fig. 4B). These results demonstrated the neuroprotective effect of OHDHA against oligomeric Aβ and NMDA-mediated excitotoxicity, and suggest that OHDHA may even induce neuronal proliferation [19].

To further investigate the mechanism by which OHDHA offers neuroprotection against oligomeric-Aβ-mediated toxicity, we carried out model membrane-based assays to analyze the binding of different aggregated forms of Aβ to lipid-raft-like vesicles composed of Cho and SM. We chose this type of vesicles because lipid-raft membrane domains have been described as the loci of Aβ generation and binding, mediating Aβ cellular toxicity [42], [53], [54]. We observed that the binding of monomeric Aβ to raft-like bilayers only occurred in the presence of OHDHA (Table 2A), while the affinity of Aβ oligomers for raft-like membranes was lower in the presence of OHDHA (ca. 8 fold reduction: Table 2B). Moreover, the affinity of Aβ fibrils for raft-like membranes was reduced by ca. 160 fold in the presence of OHDHA (an increase in the Kd value from 4.76 to 775 μM: Table 2C). These results clearly indicate that OHDHA favors the interaction of monomeric Aβ with raft-like membranes and that OHDHA impairs the interaction of oligomeric/fibrillar Aβ with membranes. These effects might explain the neuroprotection provided by OHDHA against oligomeric-Aβ-mediated toxicity in neuron-like cells (see Fig. 4A).

3.4. Evaluation of OHDHA toxicity in zebrafish embryos

The data presented here suggests that OHDHA is a therapeutic candidate for AD. For this reason, we tested the safety of OHDHA as a drug for human administration by evaluating its lethal, sub-lethal and teratogenic effects in zebrafish embryos. We tested zebrafish embryo mortality and viability on exposure to OHDHA at 1, 3, 10, 30 and 100 mg/l (2.7, 8.1, 27.3, 81.8 and 273 μM, respectively) for 24, 48 and 72 h, as well as measuring its sub-lethal and teratogenic effects. Sub-lethal effects were considered to include the lack of spontaneous movement, pigmentation deficits and edema or clots in organs or other internal structures, while teratogenic effects included deformation of organs or internal structures, scoliosis and general growth delay (see Table 3). OHDHA had only a mild effect on embryo mortality at the highest concentrations tested (100 mg/l), producing 20% mortality up to 48 h and 35% after a 72-hour exposure (Table 3A). Accordingly, embryo viability was tested at 72 h and negative effects were only produced on exposure to 100 mg/l OHDHA, whereas lower concentrations (1 to 30 mg/l) were correlated with acceptable levels of embryo viability (between 80 and 100%: Table 3B). Similarly, sub-lethal effects were only observed at high concentrations of OHDHA (100 mg/l), and in a time-dependent manner (from 56 to 77%, between 48 and 72 h), whereas no remarkable effects were observed at lower concentrations (Table 3C). It should be noted that in all cell culture experiments performed in the present work, OHDHA was used at concentrations between 5 and 30 μM. All concentrations of OHDHA appeared to produce teratogenic effects after long-term incubation (72 h), whereas only the highest concentration (100 mg/l) could induce teratogenic effects within 24 h (Table 3D). The main teratogenic effects observed were organ deformation and growth delay. However, in an elevated proportion of these embryos these effects reverted after longer exposures, even at high concentrations. Specifically, in the presence of 100 mg/l OHDHA the percentage of affected embryos decreased from 100% at 24 h to 38% at 72 h, suggesting that these teratogenic effects might be an acute response to the treatment but they were not so severe as to be maintained for an extended period.

Finally, we tested OHDHA toxicity in WT and 5xFAD mice by monitoring their weight, which increased throughout the treatment period except when they were maintained on a hypocaloric diet during the behavioral testing (Fig. S4). This result suggested that OHDHA is not toxic at therapeutic doses. Indeed, no mortality or relevant physical side-effects (hair loss, behavioral alterations like jumping or itching, etc.) were observed in association with OHDHA treatment, further suggesting that this drug is unlikely to produce toxicity when administered long-term to mice.

4. Discussion

Despite the efforts to discover a plausible and effective treatment for AD, no such therapies for this devastating disorder are as yet available. On the one hand, current therapies used for AD treatment have poor clinical efficacy, such as the administration of acetylcholinesterase inhibitors and NMDA receptor antagonists. On the other hand, drug development has mainly focused on disease-modifying strategies, such as targeting the two neuropathological features that characterize AD and that are thought

to play a central role in the neurodegeneration process: amyloid-β accumulation and tau hyperphosphorylation [55], [56]. However, these therapeutic approaches have also failed [1], including a phase III trial with the anti-Aβ antibody bapineuzumab (Pfizer, ClinicalTrials.gov reference # NCT00998764). In contrast, hydroxyl derivatives of docosahexaenoic acid have been found in nature and many of them are neuroprotective such as resolvins and protectins [20], [21], [57], [58]. In this sense, OHDHA has been shown to induce recovery of the cognitive status in an AD mouse model [19] and our present results suggest that this hydroxyl-DHA derivative constitutes a promising therapeutic alternative.

Several mechanisms have been proposed to explain the neurodegeneration associated with AD. Here, we have focused on membrane lipid changes that occur during AD as possible signals that trigger both neurodegeneration and the other neuropathological features associated with AD. In this sense, low levels of DHA and of PE, the principal phospholipid containing this fatty acid in the brain, have frequently been reported in AD [8], [9], [59], [60], [61]. However, DHA administration in patients with mild-to-moderately severe AD produced inconclusive results in clinical trials, highlighting the need to adopt different DHA-based therapeutic strategies. Here, we propose an alternative therapeutic approach based on membrane lipid targeting with OHDHA. Indeed, we previously demonstrated that OHDHA is able to improve the cognitive deficits in the 5xFAD mice (time and working/reference memory errors), as well as increasing basal neurogenesis in the hippocampus of these transgenic mice to WT levels (see Table 4) [19]. In this work, we show that OHDHA can modulate the brain membrane lipid composition by increasing the concentration of long chain PUFA-containing PE species, as well as diminishing Aβ generation in N2aSw cells and Aβ burden in the brain of 5xFAD mice. Likewise, oral administration of OHDHA inhibits tau protein phosphorylation in the brain of 5xFAD mice and in Aβ-treated neuron-like cells, and it enhances neuron-like cell viability against oligomeric-Aβ and NMDA/Ca^{2+}-mediated toxicity. Additionally, OHDHA exhibited little pharmacological toxicity in vivo, and zebrafish embryos showed no remarkable alterations in terms of mortality and sublethal effects at the doses used here.

OHDHA induced relevant lipid modifications in the brain of 5xFAD mice that were the opposite of those reported for AD. Accordingly, our lipidomic analysis showed an increase in all PE species (including diacyl-PE, lyso-PE and their plasmalogens) and in polyunsaturated acyl chains (phospholipids containing 5 or more double bonds), similar to those produced by DHA in the mouse brain [62] or in human plasma [63]. Specifically, increases in all diacyl-PE subclasses were observed, although species containing long (40C) and medium length (36–38C) acyl chains increased markedly with respect to shorter acyl chains (32–34C). It is noteworthy that OHDHA caused the highest increase in diacyl-PE 40:6 in the brain of 5xFAD mice, mainly formed by 22:6 (DHA) and 18:0 fatty acids. In addition, significant increases in other diacyl-PE subspecies were also evident in OHDHA-treated mice, such as 40:5 and 38:5, which contain the omega-3 fatty acids 22:5 (DPA) or 20:5 (EPA) and that can be generated enzymatically from the 22:6 acyl chain [62], [64]. In this context, the OHDHA-induced lipid modifications should counteract the lipid deficits associated with AD. Indeed, biopsies from AD brains were characterized by the loss of diacyl-PE subspecies (especially, 40:6, 38:6 and 38:4) and low levels of lipids containing long acyl chains, along with an increase in species containing short acyl chains in the human prefrontal cortex, among other lipid alterations [65]. Fatty acid length and their degree of saturation are determinant factors influencing membrane structure and functionality [66]. Indeed, by adequately regulating membrane lipid composition cell membranes may reverse the pathological changes in neurons, as may be the case in AD [22]. On the other hand, no remarkable differences in lipids were found in the brain of the 5xFAD AD mice compared to WT controls. However, other brain membrane lipid alterations have been detected in different AD models [65], [67] and there have been many discrepancies between post-mortem AD tissue and AD model brains, implying that AD models are likely not to faithfully reproduce all the lipid alterations associated with AD [65], [67].

We also demonstrated that OHDHA affects Aβ production in cultured cells stably expressing *Swedish* APP and in the brain of 5xFAD mice, consistent with previous observations for DHA in cultured cells and in AD models [11], [12], [68]. In this context, membrane lipids can modulate the amyloidogenic route by acting on BACE-1 and the γ-secretase complex [47], [48], [69]. The activity of these enzymes increases in raft-like domains that are enriched in Cho and SM. PE, OHDHA and PUFAs can change the membrane from a liquid ordered to a liquid disordered state, which does not support amyloidogenesis [44], [70], [71], therefore, cell membranes in the mouse brain or cultured cells that are exposed to OHDHA should undergo such changes, dampening the activity of the secretases implicated in Aβ generation. In addition, we demonstrated that OHDHA induces strong clustering of the APP, PS1 and BACE1 proteins into cellular vesicles/organelles. Although we have yet to define the nature of these

11

vesicles, these results suggest that OHDHA-induced membrane lipid changes might regulate endolysosomal proteolysis [72], and this mechanism of action may also contribute to the downregulation of Aβ after OHDHA treatment. Interestingly, autophagy/lysosomal proteolysis is impaired in AD and AD models, and its stimulation has been proposed as a potentially effective therapeutic strategy to combat AD [37], [73], [74], [75]. However, our confocal microscopy assays showed weak co-localization between APP and LC3, or APP and Lamp1, in the vesicles observed after treatment with OHDHA in N2aSw cells. Consequently, these results did not allow concluding the possible implication of the autophagy/lysosomal route as a molecular mechanism mediating downregulation of Aβ levels in OHDHA-treated N2a cells. Therefore, further analysis would be necessary to confirm this hypothesis and to identify the origin of these vesicles.

In addition, we demonstrated that OHDHA treatment protects neuron-like cells against the AD-related toxicity mediated by oligomeric Aβ or NMDA, and it prevented Aβ-induced tau hyperphosphorylation. We provided here evidence that these phenomena may be explained by the modification of membrane lipid composition and structure by OHDHA, for example the weaker affinity of oligomeric and fibrillar Aβ for raft-like vesicles containing OHDHA observed in the ITC assays. Moreover, OHDHA increases the relative abundance of polyunsaturated lipid species, which might inhibit the interaction of Aβ oligomers with lipid raft-associated protein receptors, thereby inhibiting their cytotoxic cell signaling [76]. In this context, ITC assays also demonstrated that monomeric Aβ exclusively interacted with raft-like vesicles in the presence of OHDHA, suggesting that monomeric Aβ preferentially binds to liquid disordered-prone structures [42]. Interestingly, the persistence of monomeric Aβ is associated with neuroprotection, supporting neuronal survival under conditions of trophic deprivation and combating excitotoxicity. Furthermore, monomeric Aβ enhances glycogen synthase kinase-3β (GSK-3β) phosphorylation, suggesting that monomeric Aβ may downregulate tau phosphorylation [77]. Therefore, these results suggest that OHDHA promotes neuronal survival by favoring the membrane interactions of monomeric Aβ but not those of oligomeric or fibrillar Aβ (the presence of OHDHA induces ca. 170-fold reductions in the affinity of fibrils for lipid rafts). Nevertheless, it cannot be ruled out that OHDHA may regulate APP processing by altering the membrane lipid composition, limiting the ensuing alterations originated by Aβ generation, such as Aβ oligomerization and tau hyperphosphorylation. Moreover, NMDA-mediated Ca^{2+} excitotoxicity also leads to neurodegeneration in AD [78], [79] and this may also be reversed by OHDHA. However, the molecular mechanism connecting OHDHA-mediated membrane lipid changes and NMDA-receptor trafficking at synaptic terminals remains unknown.

Interestingly, exposing differentiated neuron-like cells to OHDHA increased the proportion of viable cells in culture in the presence of a toxic insult (oligomeric Aβ or NMDA) even above that of control neuron-like cells (not submitted to toxic insult), suggesting that OHDHA might induce mitotic division of neuronal stem cells. Indeed, OHDHA induced neuronal stem cell proliferation in the hippocampus of 5xFAD mice, as reflected by a remarkable increase in the number of phospho-histone-H3-positive neurons (see Table 4) [19], although the molecular mechanisms associated with this phenomenon remain unknown. In summary, OHDHA not only has a neuroprotective influence on neuron-like cells but also, it exerts an apparent neuroregenerative effect in neuron-like cells in culture, and in the brain of 5xFAD mice, both of which might explain the enhanced cell survival, and the improved learning and memory capabilities of 5xFAD mice administered OHDHA.

AD is a complex neurodegenerative process that has been related to lipid diet and to metabolic diseases. Indeed, this pathology is probably driven by lipid alterations in neuronal membranes that lead to defective APP processing, altered cell signaling and the ensuing events characteristic of this pathology. In line with this, alterations in membrane lipids (e.g., PE and DHA) of AD patients have been described previously [65], although this fact has still not been taken into consideration when designing other therapeutic strategies. In the present work, we have investigated the molecular basis underlying the effects of OHDHA on AD-associated cognitive loss. This "membrane lipid therapy"-based drug is a molecule designed to target lipid membranes and regulates the membrane-associated protein activity, which when altered may cause neurodegeneration and eventually, AD. The beneficial effects of OHDHA include the restoration of cognitive scores in the 5xFAD model of AD, the protection of cells against external AD-associated toxic agents, such as oligomeric Aβ, and a reduction in the production of Aβ and tau hyperphosphorylation (Fig. 5). In conclusion, OHDHA constitutes a promising therapeutic compound to combat AD-associated neurodegeneration.

5. Concluding remarks

AD is a neurological disorder with unmet clinical needs. In this work, we proposed a 2-hydroxyl-derivative of DHA as a plausible alternative therapeutic strategy to treat this pathology. This drug modifies the membrane lipid composition, causing a reduction in β-amyloid production and normalization (i.e. reduction) of tau hyperphosphorylation, it enhances neuron-like cell survival and hippocampal neurogenesis, leading to improved cognitive function, as seen in the 5xFAD mouse model of Alzheimer's disease.

Conflict of interest

The authors have no conflicts of interest to declare.

Acknowledgements

Abbreviations

AD:Alzheimer's disease; APP: amyloid precursor protein; PS1:presenilin-1; Aβ: amyloid-β peptide; GFP: green fluorescent protein; WT: wild type; LC/MS: liquid chromatography/mass spectrometry; PC: phosphatidylcholine; PE: phosphatidylethanolamine; PS: phosphatidylserine; PI: phosphatidylinositol; Cho: cholesterol; SM: sphingomyelin; PUFA(s): polyunsaturated fatty acid(s); DHA: docosahexaenoic acid; EPA: eicosapentaenoic acid; DPA: docosapentaenoic acid; OHDHA: 2-hydroxydocosahexaenoic acid

References

[1] K. Mullane, M. Williams, Alzheimer's therapeutics: continued clinical failures question the validity of the amyloid hypothesis-but what lies beyond? Biochem.Pharmacol. 85 (2013) 289–305.

[2] N.E. Shepardson, G.M. Shankar, D.J. Selkoe, Cholesterol level and statin use in Alzheimer disease: I. Review of epidemiological and preclinical studies, Arch. Neurol. 68 (2011) 1239–1244.

[3] N.E. Shepardson, G.M. Shankar, D.J. Selkoe, Cholesterol level and statin use in Alzheimer disease: II. Review of human trials and recommendations, Arch. Neurol. 68 (2011) 1385–1392.

[4] J.J.M. Hoozemans, R. Veerhuis, J.M. Rozemuller, P. Eikelenboom, Soothing the inflamed brain: effect of non-steroidal anti-inflammatory drugs on Alzheimer's disease pathology, CNS Neurol. Disord. Drug Targets 10 (2011) 57–67.

[5] H.-M. Su, Mechanisms of n-3 fatty acid-mediated development and maintenance of learning memory performance, J. Nutr. Biochem. 21 (2010) 364–373.

[6] E. Kawakita, M. Hashimoto, O. Shido, Docosahexaenoic acid promotes neurogenesis in vitro and in vivo, Neuroscience 139 (2006) 991–997.

[7] N. Salem, B. Litman, H.Y. Kim, K. Gawrisch, Mechanisms of action of docosahexaenoic acid in the nervous system, Lipids 36 (2001) 945–959.

[8] G. Astarita, K.-M. Jung, N.C. Berchtold, V.Q. Nguyen, D.L. Gillen, E. Head, C.W. Cotman, D. Piomelli, Deficient liver biosynthesis of docosahexaenoic acid correlates with cognitive impairment in Alzheimer's disease, PLoS One 5 (2010) e12538.

[9] T. Fraser, H. Tayler, S. Love, Fatty acid composition of frontal, temporal and parietal neocortex in the normal human brain and in Alzheimer's disease, Neurochem. Res. 35 (2010) 503–513.

[10] D. Arsenault, C. Julien, C. Tremblay, F. Calon, DHA improves cognition and prevents dysfunction of entorhinal cortex neurons in 3xTg-AD mice, PLoS One 6 (2011) e17397.

[11] G.P. Lim, F. Calon, T. Morihara, F. Yang, B. Teter, O. Ubeda, N. Salem, S.A. Frautschy, G.M. Cole, A diet enriched with the omega-3 fatty acid docosahexaenoic acid reduces amyloid burden in an aged Alzheimer mouse model, J. Neurosci. 25 (2005) 3032–3040.

[12] M.O.W. Grimm, J. Kuchenbecker, S. Grösgen, V.K. Burg, B. Hundsdörfer, T.L. Rothhaar, P. Friess, M.C. de Wilde, L.M. Broersen, B. Penke, M. Péter, L. Vígh, H.S. Grimm, T. Hartmann, Docosahexaenoic acid reduces amyloid β production via multiple pleiotropic mechanisms, J. Biol. Chem. 286 (2011) 14028–14039.

[13] K.N. Green, H. Martinez-Coria, H. Khashwji, E.B. Hall, K.A. Yurko-Mauro, L. Ellis, F.M. LaFerla, Dietary docosahexaenoic acid and docosapentaenoic acid ameliorate amyloid-β and tau pathology via a mechanism involving presenilin 1 levels, J. Neurosci. 27 (2007) 4385–4395.

[14] M.C. Morris, D.A. Evans, J.L. Bienias, C.C. Tangney, D.A. Bennett, R.S. Wilson, N. Aggarwal, J. Schneider, Consumption of fish and n-3 fatty acids and risk of incident Alzheimer disease, Arch. Neurol. 60 (2003) 940–946.

[15] E.J. Johnson, E.J. Schaefer, Potential role of dietary n-3 fatty acids in the prevention of dementia and macular degeneration, Am. J. Clin. Nutr. 83 (2006) 1494S–1498S.

[16] Y. Freund-Levi, M. Eriksdotter-Jönhagen, T. Cederholm, H. Basun, G. Faxén-Irving, A. Garlind, I. Vedin, B. Vessby, L.O.Wahlund, J. Palmblad, Omega-3 fatty acid treatment in 174 patients with mild to moderate Alzheimer disease: OmegAD study: a randomized double-blind trial, Arch. Neurol. 63 (2006) 1402–1408.

[17] J.F. Quinn, R. Raman, R.G. Thomas, K. Yurko-Mauro, E.B. Nelson, C. Van Dyck, J.E. Galvin, J. Emond, C.R. Jack, M. Weiner, L. Shinto, P.S. Aisen, Docosahexaenoic acid supplementation and cognitive decline in Alzheimer disease: a randomized trial, JAMA 304 (2010) 1903–1911.

[18] K. Yurko-Mauro, D. McCarthy, D. Rom, E.B. Nelson, A.S. Ryan, A. Blackwell, N. Salem, M. Stedman, M. Investigators, Beneficial effects of docosahexaenoic acid on cognition in age-related cognitive decline, Alzheimers Dement. 6 (2010) 456–464.

[19] M.A. Fiol-Deroque, R. Gutierrez-Lanza, S. Terés, M. Torres, P. Barceló, R.V. Rial, A. Verkhratsky, P.V. Escribá, X. Busquets, J.J. Rodríguez, Cognitive recovery and restoration of cell proliferation in the dentate gyrus in the 5XFAD transgenicmice model of Alzheimer's disease following 2-hydroxy-DHA treatment, Biogerontology 14 (2013) 763–775.

[20] Y. Zhao, F. Calon, C. Julien, J.W. Winkler, N.A. Petasis, W.J. Lukiw, N.G. Bazan, Docosahexaenoic acid-derived neuroprotectin D1 induces neuronal survival via secretase- and PPARγ-mediated mechanisms in Alzheimer's disease models, PLoS One 6 (2011) e15816.

[21] W.J. Lukiw, J.-G. Cui, V.L. Marcheselli, M. Bodker, A. Botkjaer, K. Gotlinger, C.N. Serhan, N.G. Bazan, A role for docosahexaenoic acid-derived neuroprotectin D1 in neural cell survival and Alzheimer disease, J. Clin. Invest. 115 (2005) 2774–2783.

[22] P.V. Escribá, Membrane-lipid therapy: a new approach in molecular medicine, Trends Mol. Med. 12 (2006) 34–43.

[23] H. Oakley, S.L. Cole, S. Logan, E. Maus, P. Shao, J. Craft, A. Guillozet-Bongaarts, M. Ohno, J. Disterhoft, L. Van Eldik, R. Berry, R. Vassar, Intraneuronal beta-amyloid aggregates, neurodegeneration, and neuron loss in transgenic mice with five familial Alzheimer's disease mutations: potential factors in amyloid plaque formation, J. Neurosci. 26 (2006) 10129–10140.

[24] B.A. Wirsching, R.J. Beninger, K. Jhamandas, R.J. Boegman, S.R. El-Defrawy, Differential effects of scopolamine on working and reference memory of rats in the radial maze, Pharmacol. Biochem. Behav. 20 (1984) 659–662.

[25] E.G. Bligh, W.J. Dyer, A rapid method of total lipid extraction and purification, Can. J. Biochem. Physiol. 37 (1959) 911–917.

[26] J.M. Jiménez-López, M.P. Carrasco, C. Marco, J.L. Segovia, Hexadecylphosphocholine disrupts cholesterol homeostasis and induces the accumulation of free cholesterol in HepG2 tumour cells, Biochem. Pharmacol. 71 (2006) 1114–1121.

[27] D. Canals, D.Mormeneo, G. Fabriàs, A. Llebaria, J. Casas, A. Delgado, Synthesis and biological properties of Pachastrissamine (jaspine B) and diastereoisomeric jaspines, Bioorg. Med. Chem. 17 (2009) 235–241.

[28] A. Garanto, N.A. Mandal, M. Egido-Gabás, G. Marfany, G. Fabriàs, R.E. Anderson, J. Casas, R. Gonzàlez-Duarte, Specific sphingolipid content decrease in Cerkl knockdown mouse retinas, Exp. Eye Res. 110 (2013) 96–106.

[29] R.E. Kingston, C.A. Chen, H. Okayama, Current Protocols in Immunology, JohnWiley & Sons, Inc., 2001

[30] A. Jämsä, K. Hasslund, R.F. Cowburn, A. Bäckström,M. Vasänge, The retinoic acid and brain-derived neurotrophic factor differentiated SH-SY5Y cell line as a model for Alzheimer's disease-like tau phosphorylation, Biochem. Biophys. Res. Commun. 319 (2004) 993–1000.

[31] R.M. Gill, R. Slack, M. Kiess, P.A. Hamel, Regulation of expression and activity of distinct pRB, E2F, D-type cyclin, and CKI family members during terminal differentiation of P19 cells, Exp. Cell Res. 244 (1998) 157–170.

[32] A. Marcilla-Etxenike, M.L. Martín, M.A. Noguera-Salvà, J.M. García-Verdugo, M. Soriano-Navarro, I. Dey, P.V. Escribá, X. Busquets, 2-Hydroxyoleic acid induces ER stress and autophagy in various human glioma cell lines, PLoS One 7 (2012) e48235.

[33] M. Sastre, I. Dewachter, G.E. Landreth,T.M. Willson, T. Klockgether, F. van Leuven, M.T. Heneka, Nonsteroidal anti-inflammatory drugs and peroxisome proliferator-activated receptor-gamma agonists modulate immunostimulated processing of amyloid precursor protein through regulation of beta-secretase, J.Neurosci. 23 (2003) 9796–9804.

[34] L. Katsouri, C. Parr, N. Bogdanovic, M. Willem, M. Sastre, PPARγ co-activator-1α (PGC-1α) reduces amyloid-β generation through a PPARγ-dependent mechanism, J. Alzheimers Dis. 25 (2011) 151–162.

[35] S. Taylor, M. Wakem, G. Dijkman, M. Alsarraj, M. Nguyen, A practical approach to RT-qPCR-Publishing data that conform to the MIQE guidelines, Methods 50 (2010) S1–S5.

[36] B. Ramos, D. Baglietto-Vargas, J.C. del Rio, I. Moreno-Gonzalez, C. Santa-Maria, S. Jimenez, C. Caballero, J.F. Lopez-Tellez, Z.U. Khan, D. Ruano, A. Gutierrez, J. Vitorica, Early neuropathology of somatostatin/NPY GABAergic cells in the hippocampus of a PS1xAPP transgenic model of Alzheimer's disease, Neurobiol. Aging 27 (2006) 1658–1672.

[37] M. Torres, S. Jiménez, R. Sánchez-Varo, V. Navarro, L. Trujillo-Estrada, E. Sánchez-Mejias, I. Carmona, J.C. Davila, M. Vizuete, A. Gutiérrez, J. Vitorica, Defective lysosomal proteolysis and axonal transport are early pathogenic events that worsen with age leading to increased APP metabolism and synaptic Abeta in transgenic APP/PS1 hippocampus, Mol. Neurodegener. 7 (2012) 59.

[38] M. Gobbi, F. Re, M. Canovi, M. Beeg, M. Gregori, S. Sesana, S. Sonnino, D. Brogioli, C. Musicanti, P. Gasco, M. Salmona, M.E. Masserini, Lipid-based nanoparticles with high binding affinity for amyloid-beta1-42 peptide, Biomaterials 31 (2010) 6519–6529.

[39] L.D. Mayer, M.J. Hope, P.R. Cullis, Vesicles of variable sizes produced by a rapid extrusion procedure, Biochim. Biophys. Acta 858 (1986) 161–168.

[40] M.B. Ruiz-Argüello, G. Basáñez, F.M. Goñi, A. Alonso, Different effects of enzyme-generated ceramides and diacylglycerols in phospholipid membrane fusion and leakage, J. Biol. Chem. 271 (1996) 26616–26621.

[41] C. Arnulphi, J. Sot,M. García-Pacios, J.-L.R. Arrondo, A. Alonso, F.M.Goñi, Triton X-100 partitioning into sphingomyelin bilayers at subsolubilizing detergent concentrations: effect of lipid phase and a comparison with dipalmitoylphosphatidylcholine, Biophys. J. 93 (2007) 3504–3514.

[42] H. Ahyayauch, M. Raab, J.V. Busto, N. Andraka, J.-L.R. Arrondo, M. Masserini, I. Tvaroska, F.M. Goñi, Binding of β-amyloid (1–42) peptide to negatively charged phospholipid membranes in the liquid-ordered state: modeling and experimental studies, Biophys. J. 103 (2012) 453–463.

[43] L. Yang, N.Y. Ho, R. Alshut, J. Legradi, C. Weiss, M. Reischl, R. Mikut, U. Liebel, F. Müller, U. Strähle, Zebrafish embryos as models for embryotoxic and teratological effects of chemicals, Reprod. Toxicol. 28 (2009) 245–253.

[44] M. Ibarguren, D.J. López, J.A. Encinar, J.M. González-Ros, X. Busquets, P.V. Escribá, Partitioning of liquid-ordered/liquid-disordered membrane microdomains induced by the fluidifying effect of 2-hydroxylated fatty acid derivatives, Biochim. Biophys. Acta 1828 (2013) 2553–2563.

[45] C.Y. Shao, S.S.Mirra,H.B.R. Sait,T.C. Sacktor, E.M. Sigurdsson, Postsynaptic degeneration as revealed by PSD-95 reduction occurs after advanced Aβ and tau pathology in transgenic mouse models of Alzheimer's disease, Acta Neuropathol. 122 (2011) 285–292.

[46] S. Jawhar, A. Trawicka, C. Jenneckens, T.A. Bayer, O. Wirths, Motor deficits, neuron loss, and reduced anxiety coinciding with axonal degeneration and intraneuronal Aβ aggregation in the 5XFAD mouse model of Alzheimer's disease, Neurobiol. Aging 33 (2012) e129–140(196).

[47] P. Osenkowski,W. Ye, R. Wang, M.S.Wolfe, D.J. Selkoe, Direct and potent regulation of gamma-secretase by its lipid microenvironment, J. Biol. Chem. 283 (2008) 22529–22540.

[48] L. Kalvodova, N. Kahya, P. Schwille, R. Ehehalt, P. Verkade, D. Drechsel, K. Simons, Lipids as modulators of proteolytic activity of BACE: involvement of cholesterol, glycosphingolipids, and anionic phospholipids in vitro, J. Biol. Chem. 280 (2005) 36815–36823.

[49] Z. Amtul, M. Keet, L. Wang, P. Merrifield, D. Westaway, R.F. Rozmahel, DHA supplemented in peptamen diet offers no advantage in pathways to amyloidosis: is it time to evaluate composite lipid diet? PLoS One 6 (2011) e24094.

[50] B. De Strooper, Aph-1, Pen-2, and Nicastrin with Presenilin generate an active gamma-Secretase complex, Neuron 38 (2003) 9–12.

[51] S.L. Cole, R. Vassar, BACE1 structure and function in health and Alzheimer's disease, Curr. Alzheimer Res. 5 (2008) 100–120.

[52] C. Haass, D.J. Selkoe, Soluble protein oligomers in neurodegeneration: lessons from the Alzheimer's amyloid beta-peptide, Nat. Rev. Mol. Cell Biol. 8 (2007) 101–112.

[53] R. Williamson, A. Usardi, D.P. Hanger, B.H. Anderton, Membrane-bound β-amyloid oligomers are recruited into lipid rafts by a fyn-dependent mechanism, FASEB J. 22 (2008) 1552–1559.

[54] T. Kawarabayashi, M. Shoji, L.H. Younkin, L. Wen-Lang, D.W. Dickson, T. Murakami, E. Matsubara, K. Abe, K.H. Ashe, S.G. Younkin, Dimeric amyloid β protein rapidly accumulates in lipid rafts followed by apolipoprotein E and phosphorylated tau accumulation in the Tg2576 mouse model of Alzheimer's disease, J. Neurosci. 24 (2004) 3801–3809.

[55] B. De Strooper, R. Vassar, T. Golde, The secretases: enzymes with therapeutic potential in Alzheimer disease, Nat. Rev. Neurol. 6 (2010) 99–107.

[56] C. Gao, C. Hölscher, Y. Liu, L. Li, GSK3: a key target for the development of novel treatments for type 2 diabetes mellitus and Alzheimer disease, Rev. Neurosci. 23 (2012) 1–11.

[57] B.D. Levy, Resolvins and protectins: natural pharmacophores for resolution biology, Prostaglandins Leukot. Essent. Fatty Acids 82 (2010) 327–332.

[58] K.H. Weylandt, C.-Y. Chiu, B. Gomolka, S.F. Waechter, B. Wiedenmann, Omega-3 fatty acids and their lipid mediators: towards an understanding of resolvin and protectin formation, Prostaglandins Other Lipid Mediat. 97 (2012) 73–82.

[59] M. Söderberg, C. Edlund, K. Kristensson, G. Dallner, Fatty acid composition of brain phospholipids in aging and in Alzheimer's disease, Lipids 26 (1991) 421–425.

[60] Z. Guan, Y. Wang, N.J. Cairns, P.L. Lantos, G. Dallner, P.J. Sindelar, Decrease and structural modifications of phosphatidylethanolamine plasmalogen in the brain with Alzheimer disease, J. Neuropathol. Exp. Neurol. 58 (1999) 740–747.

[61] M.R. Prasad, M.A. Lovell, M. Yatin, H. Dhillon, W.R. Markesbery, Regional membrane phospholipid alterations in Alzheimer's disease, Neurochem. Res. 23 (1998) 81–88.

[62] J.T. Wood, J.S. Williams, L. Pandarinathan, D.R. Janero, C.J. Lammi-Keefe, A. Makriyannis, Dietary docosahexaenoic acid supplementation alters select physiological endocannabinoid-system metabolites in brain and plasma, J. Lipid Res. 51 (2010) 1416–1423.

[63] I. Ottestad, S. Hassani, G.I. Borge, A. Kohler, G. Vogt, T. Hyötyläinen, M. Orešič, K.W. Brønner, K.B. Holven, S.M. Ulven, M.C.W. Myhrstad, Fish oil supplementation alters the plasma lipidomic profile and increases long-chain PUFAs of phospholipids and triglycerides in healthy subjects, PLoS One 7 (2012) e42550.

[64] M. Grønn, E. Christensen, T.A. Hagve, B.O. Christophersen, Peroxisomal retroconversion of docosahexaenoic acid (22:6(n-3)) to eicosapentaenoic acid (20:5(n-3)) studied in isolated rat liver cells, Biochim. Biophys. Acta 1081 (1991) 85–91.

[65] R.B. Chan, T.G. Oliveira, E.P. Cortes, L.S. Honig, K.E. Duff, S.A. Small, M.R. Wenk, G. Shui, G. Di Paolo, Comparative lipidomic analysis of mouse and human brain with Alzheimer disease, J. Biol. Chem. 287 (2012) 2678–2688.

[66] A.A. Spector, M.A. Yorek, Membrane lipid composition and cellular function, J. Lipid Res. 26 (1985) 1015–1035.

[67] Y. Tajima, M. Ishikawa, K.Maekawa,M.Murayama, Y. Senoo, T. Nishimaki-Mogami,H. Nakanishi, K. Ikeda, M. Arita, R. Taguchi, A. Okuno, R. Mikawa, S. Niida, O. Takikawa, Y. Saito, Lipidomic analysis of brain tissues and plasma in amousemodel expressingmutated human amyloid precursor protein/tau for Alzheimer's disease, Lipids Health Dis. 12 (2013) 68.

[68] C. Sahlin, F.E. Pettersson, L.N.G. Nilsson, L. Lannfelt, A.-S. Johansson, Docosahexaenoic acid stimulates non-amyloidogenic APP processing resulting in reduced Abeta levels in cellular models of Alzheimer's disease, Eur. J. Neurosci. 26 (2007) 882–889.

[69] O. Holmes, S. Paturi, W. Ye, M.S. Wolfe, D.J. Selkoe, Effects of membrane lipids on the activity and processivity of purified γ-secretase, Biochemistry 51 (2012) 3565–3575.

[70] S.R. Shaikh, Biophysical and biochemical mechanisms by which dietary N-3 polyunsaturated fatty acids from fish oil disrupt membrane lipid rafts, J. Nutr. Biochem. 23 (2012) 101–105.

[71] K.S. Vetrivel, G. Thinakaran, Membrane rafts in Alzheimer's disease beta-amyloid production, Biochim. Biophys. Acta 1801 (2010) 860–867.

[72] H. Schulze, T. Kolter, K. Sandhoff, Principles of lysosomal membrane degradation: cellular topology and biochemistry of lysosomal lipid degradation, Biochim. Biophys. Acta 1793 (2009) 674–683.

[73] R.A. Nixon, J.Wegiel, A. Kumar,W.H. Yu, C. Peterhoff, A. Cataldo, A.M. Cuervo, Extensive involvement of autophagy in Alzheimer disease: an immuno-electron microscopy study, J. Neuropathol. Exp. Neurol. 64 (2005) 113–122.

[74] R. Sanchez-Varo, L. Trujillo-Estrada, E. Sanchez-Mejias, M. Torres, D. Baglietto-Vargas, I. Moreno-Gonzalez, V. De Castro, S. Jimenez, D. Ruano, M. Vizuete, J.C. Davila, J.M. Garcia-Verdugo, A.J. Jimenez, J. Vitorica, A. Gutierrez, Abnormal accumulation of autophagic vesicles correlates with axonal and synaptic pathology in young Alzheimer's mice hippocampus, Acta Neuropathol. 123 (2012) 53–70.

[75] V. Schaeffer, I. Lavenir, S. Ozcelik, M. Tolnay, D.T.Winkler,M. Goedert, Stimulation of autophagy reduces neurodegeneration in a mouse model of human tauopathy, Brain 135 (2012) 2169–2177.

[76] J.V. Rushworth, H.H. Griffiths, N.T. Watt, N.M. Hooper, Prion protein-mediated toxicity of amyloid-β oligomers requires lipid rafts and the transmembrane LRP1, J. Biol. Chem. 288 (2013) 8935–8951.

[77] M.L. Giuffrida, F. Caraci, B. Pignataro, S. Cataldo, P. De Bona, V. Bruno, G.Molinaro, G. Pappalardo, A. Messina, A. Palmigiano, D. Garozzo, F. Nicoletti, E. Rizzarelli, A. Copani, Beta-amyloid monomers are neuroprotective, J. Neurosci. 29 (2009) 10582–10587.

[78] R. Resende, C. Pereira, P. Agostinho, A.P. Vieira, J.O.Malva, C.R. Oliveira, Susceptibility of hippocampal neurons to Abeta peptide toxicity is associated with perturbation of Ca2+ homeostasis, Brain Res. 1143 (2007) 11–21.

[79] L. Texidó, M. Martín-Satué, E. Alberdi, C. Solsona, C. Matute, Amyloid β peptide oligomers directly activate NMDA receptors, Cell Calcium 49 (2011) 184–190

Table 1. LC/MS characterization of diacyl-PE acyl chains in the brain of OHDHA-treated 5xFAD mice

Diacyl-PE subspecies		WT		5xFAD				5xFAD + OHDHA			
		Mean[a]	SEM[a]	Mean[a]	SEM[a]	% change[b]		Mean[a]	SEM[a]	% change[b]	
Short acyl chains	32:0	112	3	105	3	− 6.3 ± 3.0	NS	134	3	19.6 ± 3.0	**
	32:1	168	4	205	39	22.2 ± 22.9	NS	240	13	42.5 ± 7.7	NS
	34:1	2197	148	1817	71	− 17.3 ± 3.2	NS	3030	188	37.9 ± 8.5	**
	34:2	326	25	372	71	14.4 ± 21.7	NS	402	17	23.5 ± 5.4	NS
	Subtotal	2803	154	2500	85	− 10.7 ± 3.0	NS	**3805**	**216**	**35.7 ± 7.7**	**
Medium acyl chains	36:1	3862	477	3332	185	− 13.7 ± 4.8	NS	5426	204	40.5 ± 5.3	**
	36:2	3108	195	2584	98	− 16.9 ± 3.2	NS	4319	210	39.0 ± 6.8	**
	36:3	274	30	254	27	− 7.2 ± 9.9	NS	303	22	10.4 ± 8.2	NS
	36:4	3184	454	3416	465	7.3 ± 14.6	NS	5390	352	69.3 ± 11.0	*
	36:5	201	16	318	69	58.8 ± 34.6	NS	295	11	46.9 ± 5.5	*
	38:1	588	12	441	50	− 24.9 ± 8.5	NS	713	53	21.4 ± 9.0	*
	38:2	547	18	389	6	− 28.8 ± 1.0	*	593	57	8.5 ± 10.4	NS
	38:4	16,804	2171	16,670	1969	− 0.8 ± 11.7	NS	24,716	1072	47.1 ± 6.4	*
	38:5	2799	135	2903	143	3.7 ± 5.1	NS	4579	90	63.6 ± 3.2	***
	38:6	13,444	2330	12,244	821	− 8.9 ± 6.1	NS	16,532	1412	23.0 ± 10.5	NS
	38:7	244	30	340	100	38.9 ± 40.8	NS	425	19	73.7 ± 7.6	NS
	Subtotal	45,054	5749	42,891	3716	− 4.8 ± 8.2	NS	**63,290**	**3171**	**40.4 ± 7.0**	*
Long acyl chains	40:1	174	13	106	17	− 38.9 ± 9.7	NS	160	23	− 8.0 ± 13.0	NS
	40:3	2768	369	2764	315	− 0.2 ± 11.4	NS	4121	257	48.9 ± 9.3	NS
	40:5	26,517	3064	26,194	2062	− 1.2 ± 7.8	NS	38,945	2170	46.9 ± 8.2	*
	40:6	3289	896	3901	785	18.6 ± 23.9	NS	6089	286	85.2 ± 8.7	*
	Subtotal	32,747	4196	32,964	3137	0.7 ± 9.6	NS	**49,314**	**2633**	**50.5 ± 8.0**	*
Total		80,605	10,036	78,356	6833	− 2.8 ± 8.5	NS	**116,411**	**10,334**	**44.4 ± 7.4**	*

Multiple statistical analysis was performed with one-way ANOVA & Tukey's post hoc test. NS: not significant, * $p < 0.05$, ** $p < 0.01$ and *** $p < 0.001$.

[a] The measure of diacyl-PE subspecies (mean ± SEM) shown as pmol of lipid/mg of protein.

[b] The relative change in 5xFAD or OHDHA-treated 5xFAD brains relative to the mean WT value is shown as the mean ± SEM.

Table 2. OHDHA incorporation into lipid raft-like vesicles inhibits binding of Aβ oligomers and fibrils.

Empty Cell	SM/Cho/OHDHA [a]	SM/Cho [a]
Empty Cell	**(1:1:0.1 mol ratio)**	**(1:1 mol ratio)**
A. Monomer		
Kd (μM)[b]	58 ± 7.7	No interaction
ΔH (Kcal/mol)[b]	− 3.31 ± 0.24	detected
ΔS (cal/mol.°C)[b]	8.7 ± 0.5	–
ΔG (Kcal/mol)[b]	− 6.01 ± 0.40	–
B. Oligomer		
Kd (μM)[b]	21.6 ± 2.8 ***	2.7 ± 0.9
ΔH (Kcal/mol)[b]	− 1.06 ± 0.98 **	− 2.11 ± 0.09
ΔS (cal/mol.°C)[b]	17.9 ± 3.2	18.6 ± 2.5
ΔG (Kcal/mol)[b]	− 6.61 ± 1.10	− 7.80 ± 0.40
C. Fibrils		
Kd (μM)[b]	775 ± 52 ***	4.76 ± 0.11
ΔH (Kcal/mol)[b]	− 2.77 ± 0.24 ***	− 0.87 ± 0.06
ΔS (cal/mol.°C)[b]	5.3 ± 0.9 **	21.6 ± 1.2
ΔG (Kcal/mol)[b]	− 4.41 ± 1.00 *	− 7.56 ± 1.50

The data are expressed as the mean ± SEM. Statistical analysis was performed by two-tailed *t*-test: * *p < 0.05*, ** *p < 0.01* and *** *p < 0.001*.

a
Large unilamellar vesicles composed of SM and Cho, plus/minus OHDHA, were used for isothermal calorimetric titration, together with different forms of Aβ42 peptide: (A) monomeric, (B) oligomeric and (C) fibrillar (n = 3).

b
The parameters measured in the assay: Kd (dissociation constant), ΔH (enthalpy change), ΔS (entropy change) and ΔG (Gibbs free energy change) were obtained as described in the Section 2.9.

Table 3. Evaluation of OHDHA toxicity in zebrafish embryos.

OHDHA (mg/ml)	Incubation (h)		
	24	48	72
A. Embryo mortality			
1	0	0	0
3	0	0	0
10	0	0	0
30	0	0	10
100	20	20	35
B. Embryo viability			
1	–	–	100
3	–	–	80
10	–	–	80
30	–	–	94
100	–	–	46
C. Sublethal effects			
1	0	0	0
3	0	0	0
10	0	5	5
30	0	10	0
100	0	56	77
D. Teratogenic effects			
1	0	0	5
3	0	0	70
10	5	5	50
30	10	25	100
100	100	66	38

The data are expressed as the percentage of embryos that showed any of the parameters studied: (A) embryo mortality, (B) embryo viability, (C) sub-lethal effects: lack of spontaneous movements, pigmentation deficits and apparition of edema or clots in internal structures, and (D) teratogenic effects: deformation of internal structures, scoliosis and general growth delay.

Table 4. Improved cognition and neurogenesis in OHDHA-treated-5xFAD mice.

Empty Cell	WT	5xFAD			5xFAD + OHDHA		
	mean ± SEM	mean ± SEM	% change[a]		mean ± SEM	% change[b]	
Time (s) [c]	75.69 ± 4.77	124.4 ± 12.38	64.35 ± 9.95	**	105.4 ± 10.34	− 15.27 ± 9.81	NS
WME (number of errors) [c]	2.32 ± 0.32	3.95 ± 0.47	70.25 ± 11.89	*	2.21 ± 0.40	− 44.05 ± 18.09	§
RME (number of errors) [c]	5.88 ± 0.39	8.31 ± 0.64	41.32 ± 7.70	*	6.07 ± 0.73	− 26.94 ± 12.02	§
Phospho histone-H3 positive neurons (cells/mm^3)[d]	7431 ± 1918	1970 ± 767.1	− 73.48 ± 38.93	*	5374 ± 939.7	272.79 ± 17.47	§

The statistical analysis was performed with a two-tailed *t*-test: * *p < 0.05* and ** *p < 0.01* after comparison between WT and 5xFAD; NS: not significant and § *p < 0.05* comparing OHDHA-treated-5xFAD and 5xFAD control mice. Summary of data extracted from [19].

[a] Percentage change in 5xFAD control mice was expressed as the mean ± SEM relative to the WT as a reference.

[b] The percentage change in 5xFAD + OHDHA was expressed as the mean ± SEM relative to 5xFAD mice.

[c] Time (s), and the number of working and reference memory errors (WME and RME, respectively) were determined during the radial arm maze test (WT, n = 10; 5xFAD, n = 11 and 5xFAD + OHDHA, n = 12).

[d] Neuronal proliferation in the dentate gyrus (hippocampus) was determined by quantifying the number of phospho-histone H3-positive neurons in the granullar cell layer of immunolabeled brain sections (WT, n = 4; 5xFAD n = 7 and 5xFAD + OHDHA, n = 7).

Figure legends

Figure 1. Effect of OHDHA on membrane lipid composition in the brain of 5xFAD mice. Bar diagrams show the relative change in lipids in OHDHA-treated (dark gray bars) and control 5xFAD mice (light gray bars) compared to the WT (considered as 100%, filled bars). LC/MS was used to analyze the levels of: (A) phosphatidylethanolamine (diacyl-PE, lyso-PE and their plasmalogens), (B) polyunsaturated phospholipids (containing 5 or more double bonds), (C) saturated phospholipids, (D) phosphatidylcholine (diacyl-PC, lyso-PC and their plasmalogens), (E) phosphatidylinositol (diacyl-PI), (F) phosphatidylserine (diacyl-PS and lyso-PS), (H) sphingolipids (sphingomyelin and dihydrosphingomyelin) and (I) ceramides (ceramide, lactosyl-ceramide and hexosyl-ceramides); and (G) cholesterol levels were determined by an enzymatic colorimetric method. These data showed a significant increase in PE, PI and PUFA-containing phospholipids in OHDHA-treated 5xFAD mice compared with 5xFAD and WT control mice (panels A, B and E, respectively). No remarkable differences between 5xFAD and WT samples were observed for any of the lipids studied. Bars show the mean value from 3 animals ± SEM and the statistical analysis was performed by one-way ANOVA and Tukey's post hoc multiple comparison: *, $p < 0.05$.

Figure 2. OHDHA diminishes the β-amyloid brain pathology and tau hyperphosphorylation. (A) Representative western blots showing monomeric Aβ, phospho-tau (Ser-202; CP13 epitope) and total tau (Tau46) in 5xFAD brain samples (same mice used in Fig. 1) with tubulin-α used as a loading control (upper panel). Western blot quantification showed a significant decrease in Aβ in the brain of 5xFAD mice that received OHDHA (middle panel). In the same way, quantification of phospho and total tau revealed a significant increase in phospho-tau levels in 5xFAD that was majorly prevented in OHDHA-treated 5xFAD mice, as compared with WT, whereas total-tau levels did not show any significant differences. Consequently, the phospho/total tau ratio was showed significantly increased in 5xFAD but not in OHHDA-treated 5xFAD mice, as compared with WT (lower panel) (bars show the mean value from 3 animals ± SEM). (B) Representative western blot of Aβ and sAPPα in N2aSw cell culture media (upper panel). Western blot quantification revealed that exposing N2aSw cells to OHDHA (10 μM) for 24 h drastically reduced Aβ production without altering sAPPα levels (n = 3) (lower panel). (C) Representative western blot of tau hyperphosphorylation in neuron-like differentiated SH-SY5Y cells (upper panel). Western blot quantification showed a strong induction of tau phosphorylation at the AT8 epitope after Aβ stimulation, whereas addition of OHDHA (5 μM) partly reduced Aβ-mediated tau phosphorylation and it was completely abolished in the presence of OHDHA (10 μM; n = 3) (lower panel). #, $p < 0.05$ according to two-tailed *t*-test between two groups; *, $p < 0.05$ according to multiple statistical analysis by one-way ANOVA and Tukey's post hoc test.

Figure 3. Subcellular distribution of APP, PS1 and BACE1 in N2aSw (APPsw) and MDCK (APP-GFP) cell cultures treated with OHDHA. (A) Confocal images showing N2a cells stably expressing *Swedish* APP. Cells were immunolabeled with the 6E10 antibody to detect APP (panels A1–A2), with an anti-BACE1 antibody (panels A5–A6) or transfected with a PS1-GFP vector (panels A3–A4). Immunofluorescence assays showed APP, BACE-1 and PS1 cluster in cell vesicles/organelles following OHDHA treatment (panels A2, A4 and A6, respectively) as compared to control cells (panels A1, A3 and A5, respectively). (B) Confocal images of MDCK cells stably expressing APP-GFP and exposed to increasing concentrations of OHDHA (B1: 10 μM; B2: 15 μM; B3: 20 μM; B4: 25 μM). Vesicular accumulation of APP-GFP confirmed previous results with N2aSw cells (panel A2). APP clustering was evident in the presence of OHDHA (10 μM) and the number of GFP-positive vesicles rapidly increased at higher concentrations until saturation. Fluorescent vesicle quantification showed an EC_{50} value of 17.8 μM (B5). Scale bars: 10 μm (A1–A6) and 20 μm (B1–B4).

Figure 4. Fig. 4. OHDHA protected cells with a neuron-like phenotype against an Aβ or a NMDA-mediated toxic insult. (A) SH-SY5Y cells were differentiated into neuron-like cells and treated with oligomeric Aβ peptide (5 μM) for 24 h in the presence or absence of OHDHA (5 and 10 μM). The MTT assay was used to quantify the number of viable cells/well. Oligomeric Aβ reduced cell viability but the number of viable cells was recovered upon OHDHA treatment to the untreated control values (5 μM OHDHA) or even higher (10 μM OHDHA; n = 3). (B) P19 embryonic stem cells were differentiated into neuron-like cells and exposed to NMDA (in the presence of 10 mM Ca^{2+}). Concomitant OHDHA treatment reduced NMDA/Ca^{2+}-induced cell death and even increased the number of viable cells above that of the untreated controls (n = 3). #, $p < 0.05$ according to two-tailed *t*-test between two groups; *, $p < 0.05$ compared to Aβ- or NMDA-treated controls, according to multiple statistical analysis by one-way ANOVA and Tukey's post hoc test.

Figure 5. Postulated mechanism of action for OHDHA. Summary of the proposed molecular mechanisms underlying the effects of OHDHA on neuronal membranes. OHDHA enriches brain membranes in PE, especially those carrying DHA and other long PUFAs. These lipid changes may influence the structure of the cell membrane, leading to the formation of liquid-disordered-prone structures, and they might reverse the cellular signaling associated with AD by: (i) downregulating amyloidogenic processing and Aβ-dependent tau protein hyperphosphorylation; and (ii) decreasing neuron vulnerability to extracellular toxic agents such as oligomeric Aβ and NMDA/Ca^{2+}-mediated excitotoxicity. In addition, OHDHA also induced proliferation of both neuron-like cells in vitro and neuron stem cells in the mouse brain. Together, this evidence supports a neuroprotective and neuroregenerative role of OHDHA that may be associated with the improved cognitive capabilities seen in the 5xFAD mouse model.

Figure S1. Relative abundance of lipid species in the brain of WT, 5XFAD and OHDHA-treated 5xFAD mice. The data are expressed as the percentage of one lipid species relative to the total lipids studied in the mouse brain. The PE family (diacyl-PE, lysoPE and their alkyl/alkenyl-plasmalogens) is the most abundant, followed by Cho, diacyl-PC and SM. OHDHA-treated 5xFAD mice showed higher levels of all PE species while other species such as Cho, diacyl-PC and SM were slightly diminished as a consequence of the high PE levels compared to WT and 5xFAD control mice. Bars show the mean value from 3 animals ± SEM.

Figure S2. Mouse and human APP expression in the brain of WT and 5xFAD mice. The genetic expression of mouse (mAPP) and human APP (hAPP) was determined by real time PCR using specific primers. Expression of hAPP was exclusively detected in 5xFAD mice and no remarkable differences were found between OHDHA-treated and 5xFAD control mice. Additionally, expression of the human gene was higher than that of mAPP in 5xFAD mice. Bars show the mean value from 3 animals ± SEM: *, $p < 0.05$ according to multiple statistical analysis by one-way ANOVA and Tukey's post hoc test.

Figure S3. Cellular co-localization of APP and LC3/Lamp1 in N2aSw (APPsw) cell cultures treated with OHDHA. Confocal images showing N2a cells stably expressing *Swedish* APP. Double immunofluorescence labeling using mouse anti-APP (clone 6E10; panel A1) and rabbit anti-LC3 (autophagic vesicle marker; panel A2), or well, rabbit anti-APP C-terminal (R1(57); panel B1) and mouse anti-Lamp1 (lysosomal marker; panel B2), and confocal laser microscopy demonstrated weak co-localization of both APP/LC3 (panel A3) or APP/Lamp1 (panel B3) in the same APP-positive vesicles accumulated after OHDHA treatment (10 μM, 24 h). Scale bars: 10 μm.

Figure S4. Weight of control and OHDHA-treated mice. The weight of the animals was monitored three times a week for the whole period of treatment with OHDHA (or vehicle alone, controls). All mice increased their weight during the treatment until they started the hypocaloric diet necessary to perform the radial arm maze test (4th month). The data are presented as the percentage change relative to the first day of treatment. Each point shows the mean value from 3 animals ± SEM.
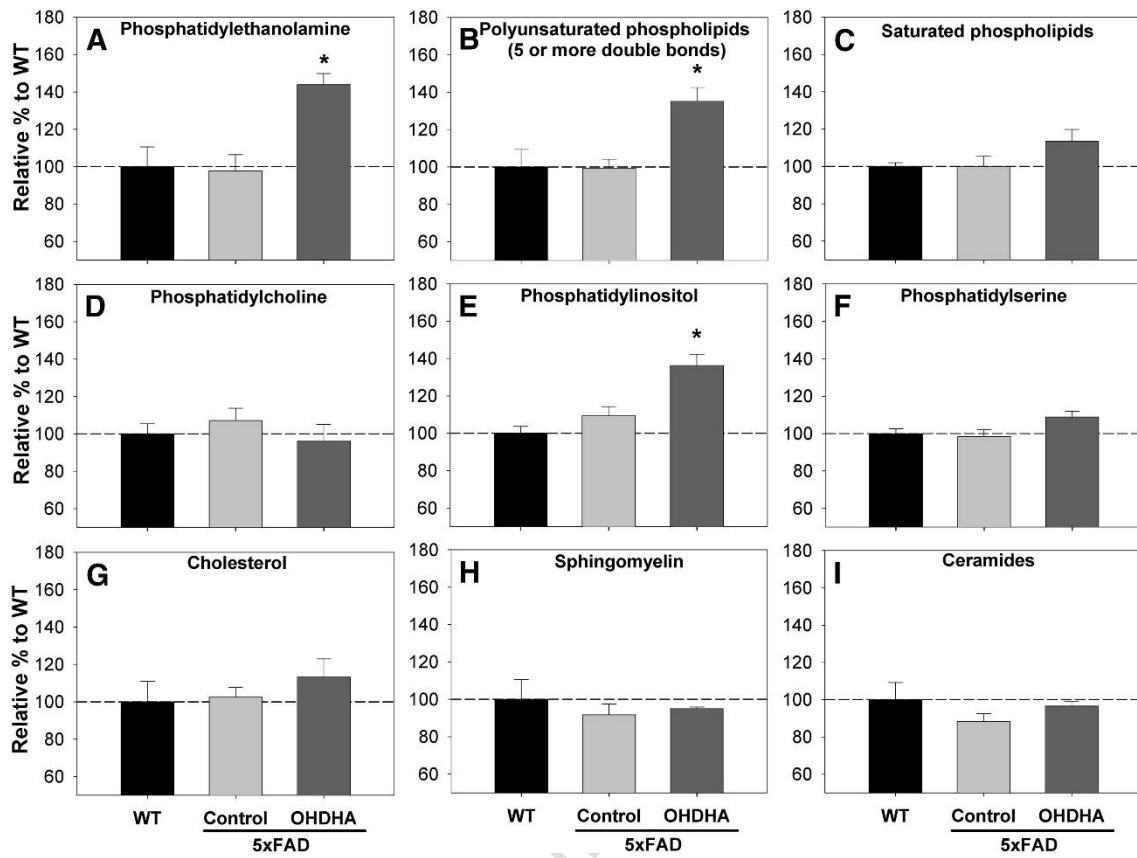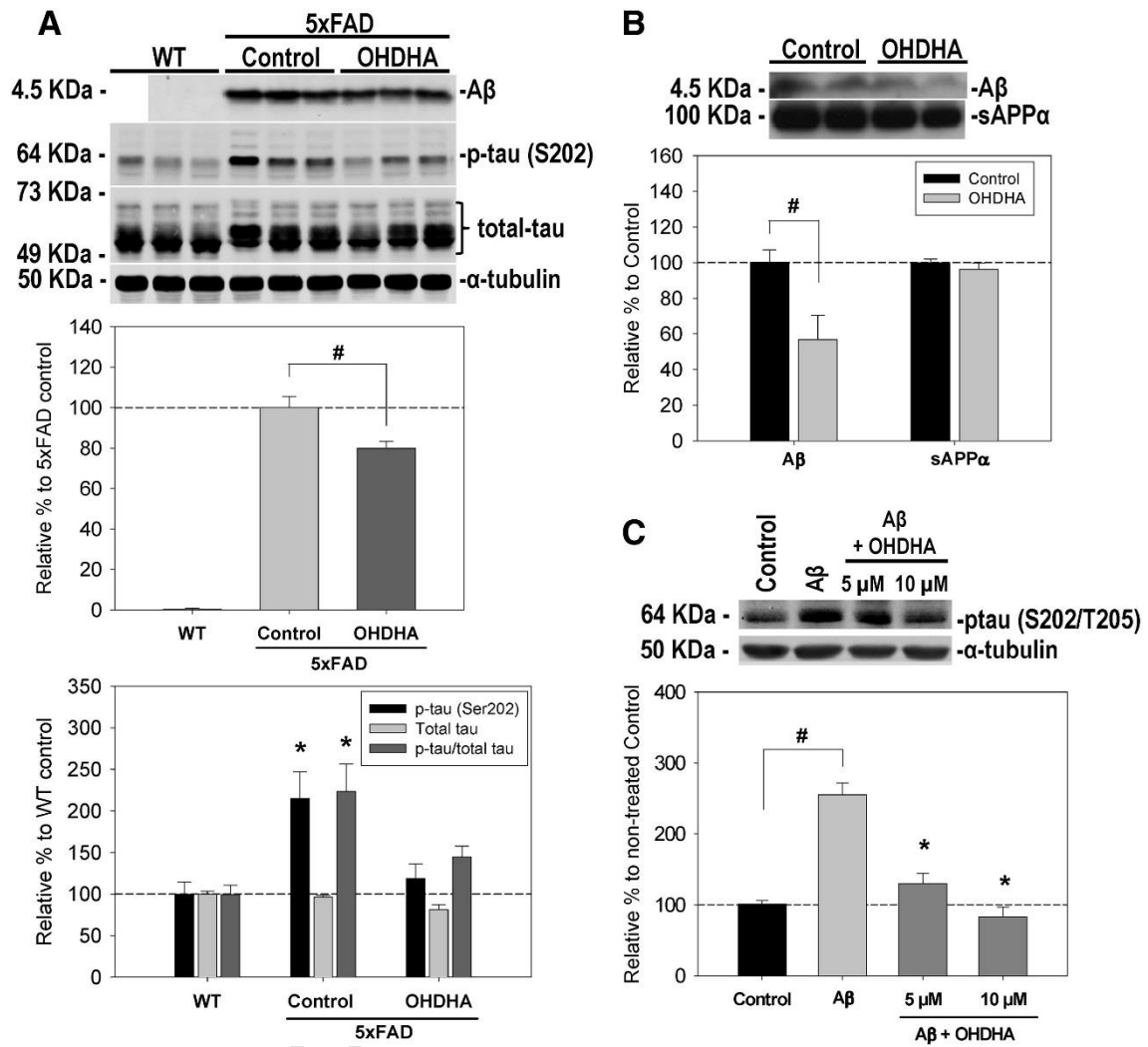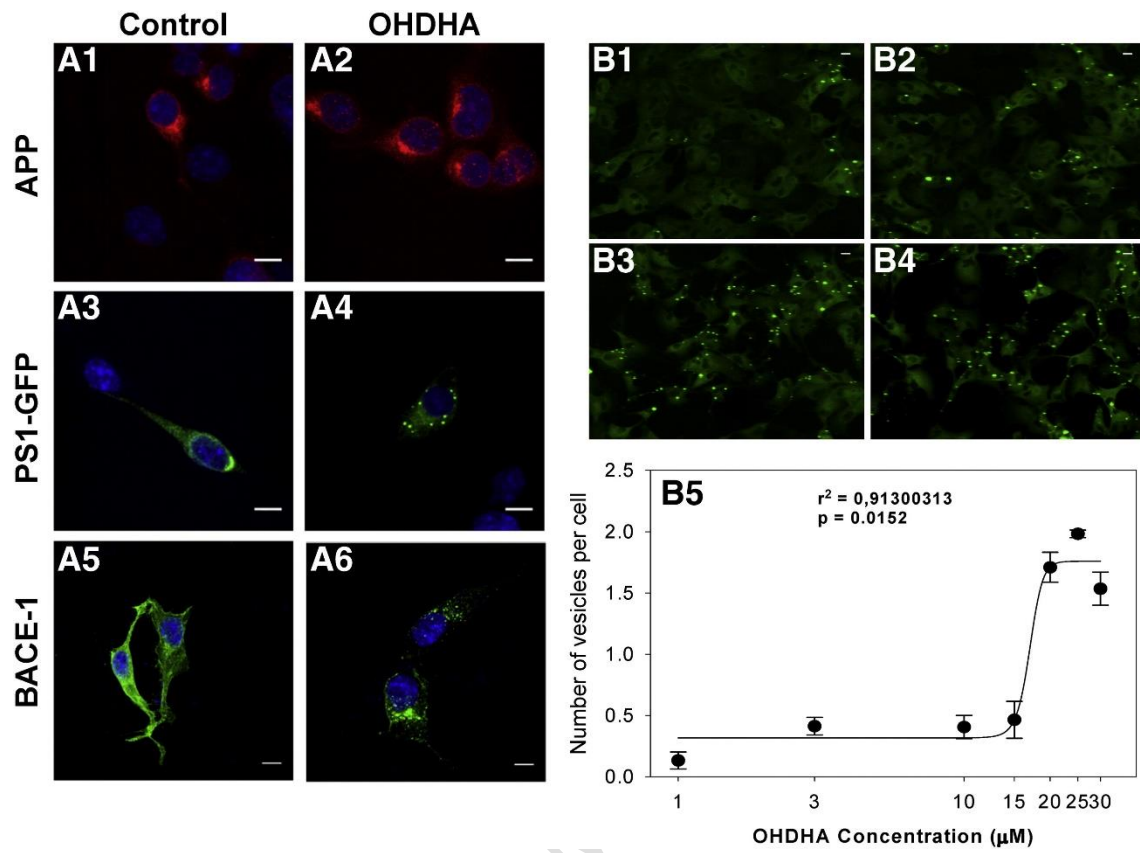
Figure 1

Figure 2

Figure 3

A

SH-SY5Y viable cells Relative % to Control

200

150

100

50

0

#

*

*

Control   Aβ   5 µM   10 µM

Aβ + OHDHA

B

P19 viable cells Relative % to control

250

200

150

100

50

0

#

*

Control   Control   OHDHA

NMDA + Ca^{2+}
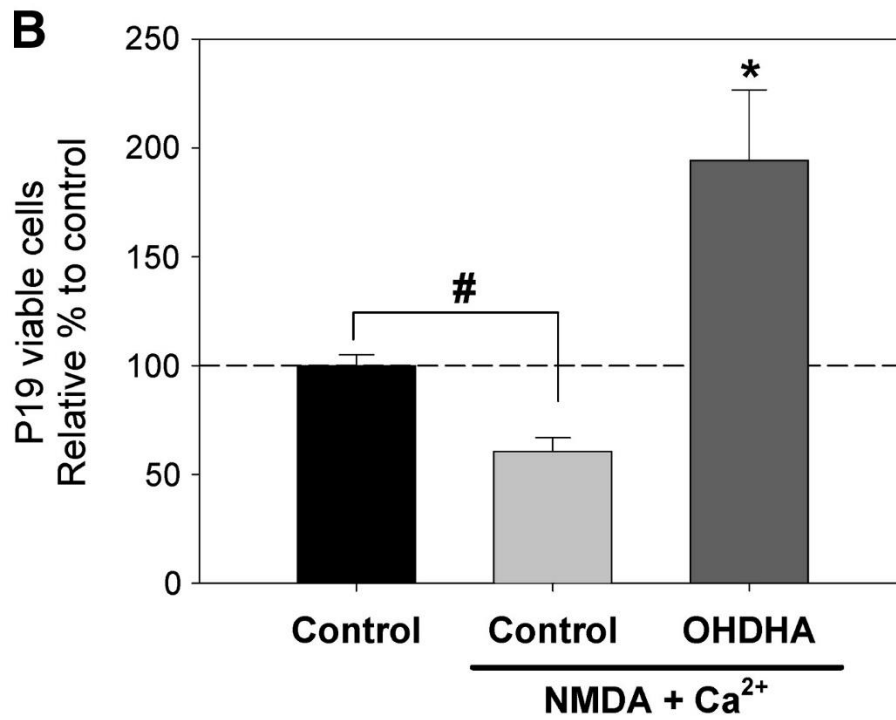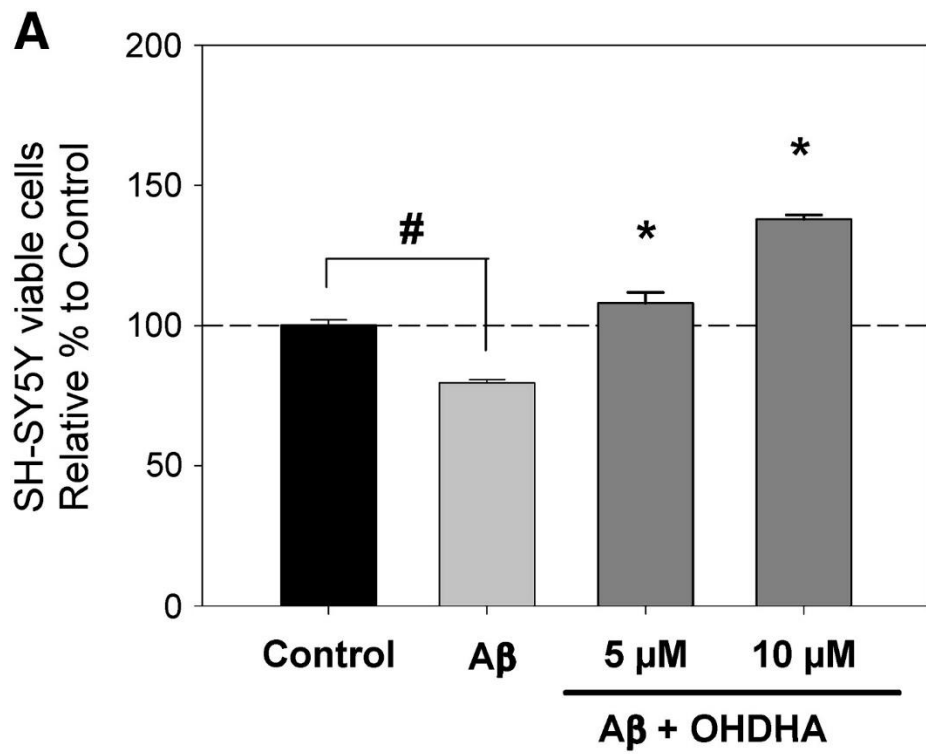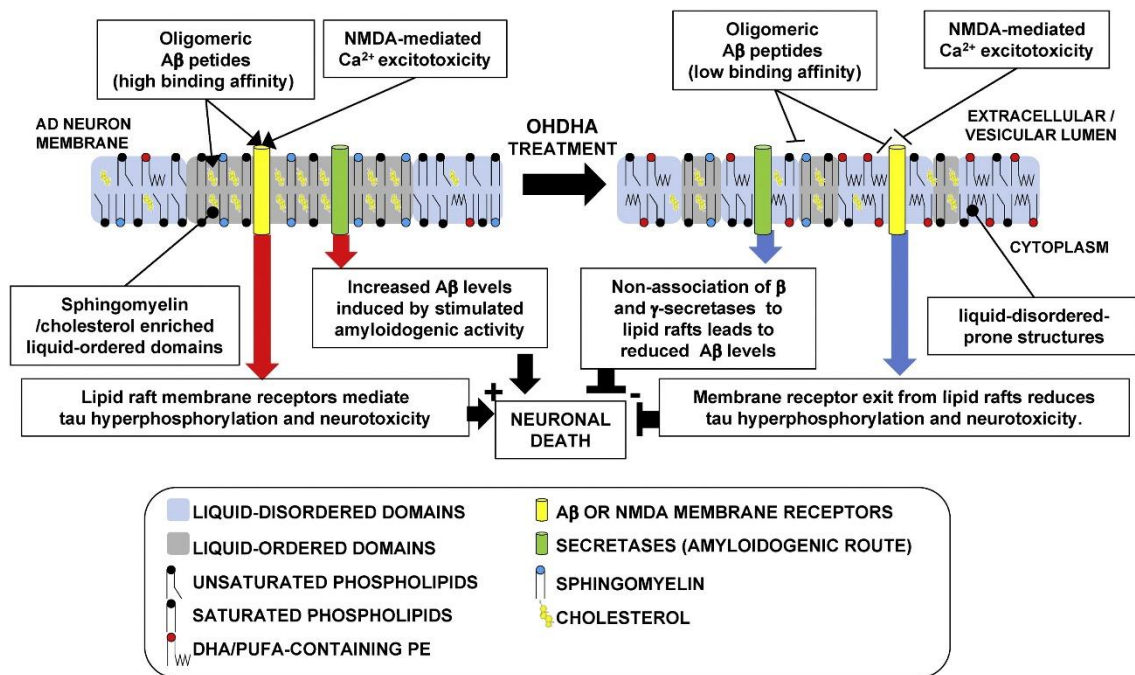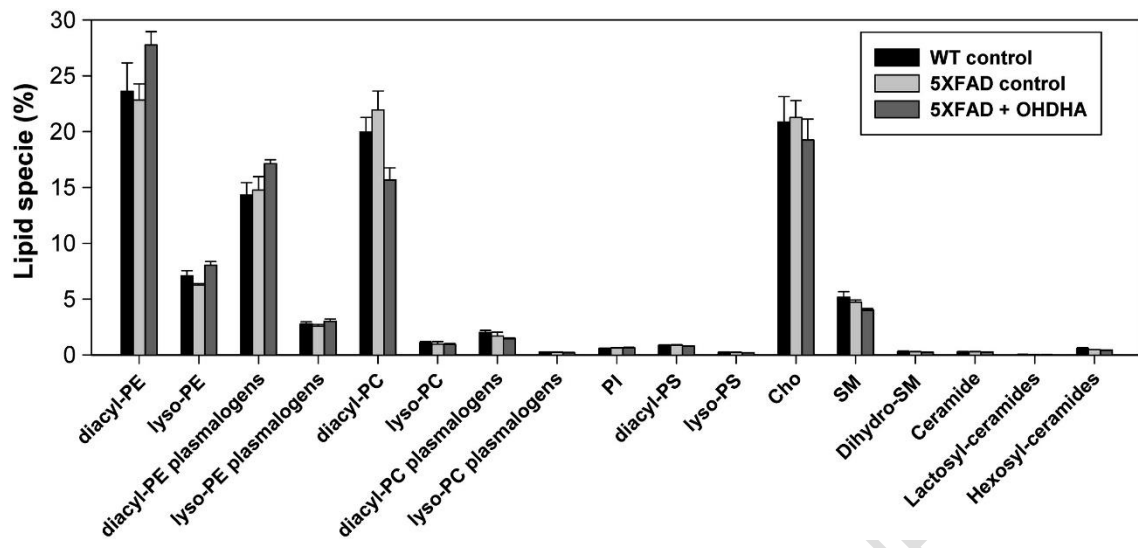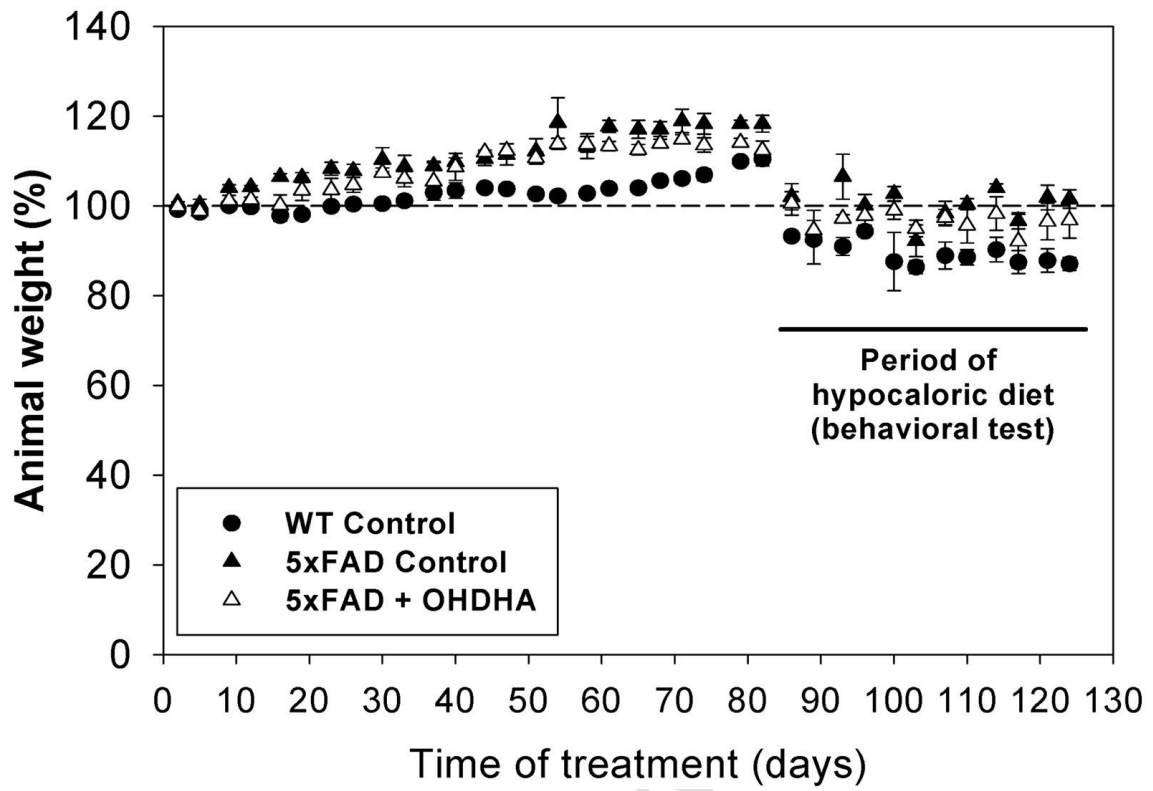
Figure 4

Figure 5

Figure S1
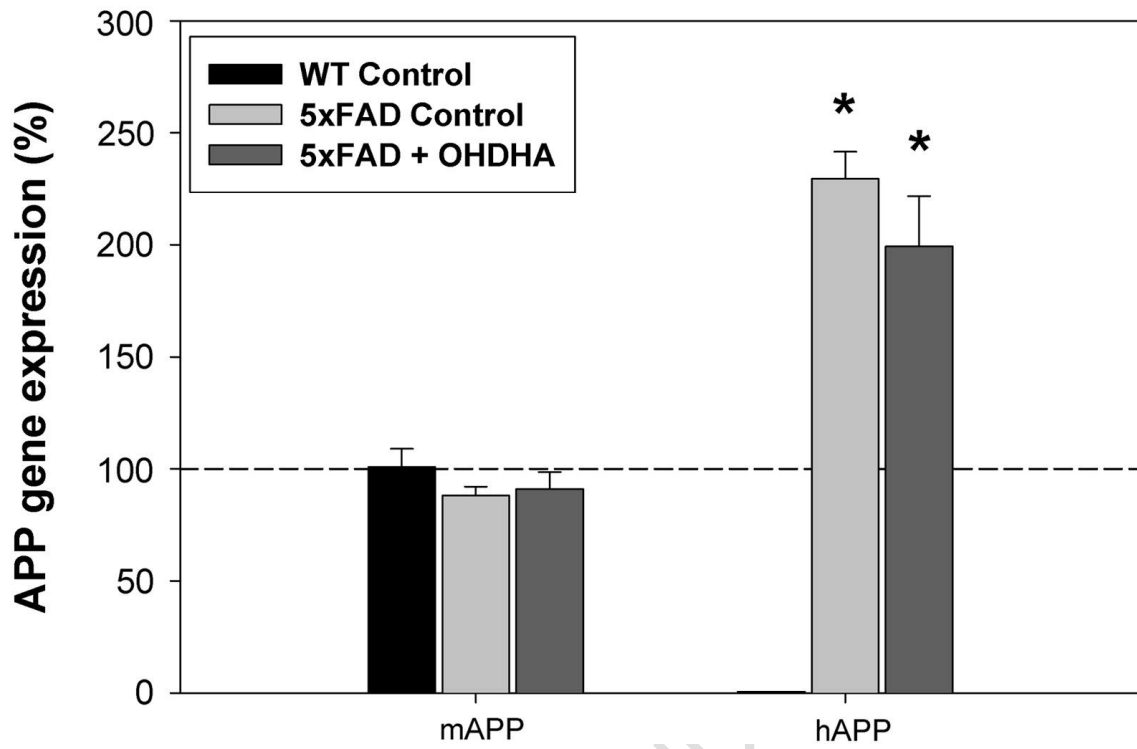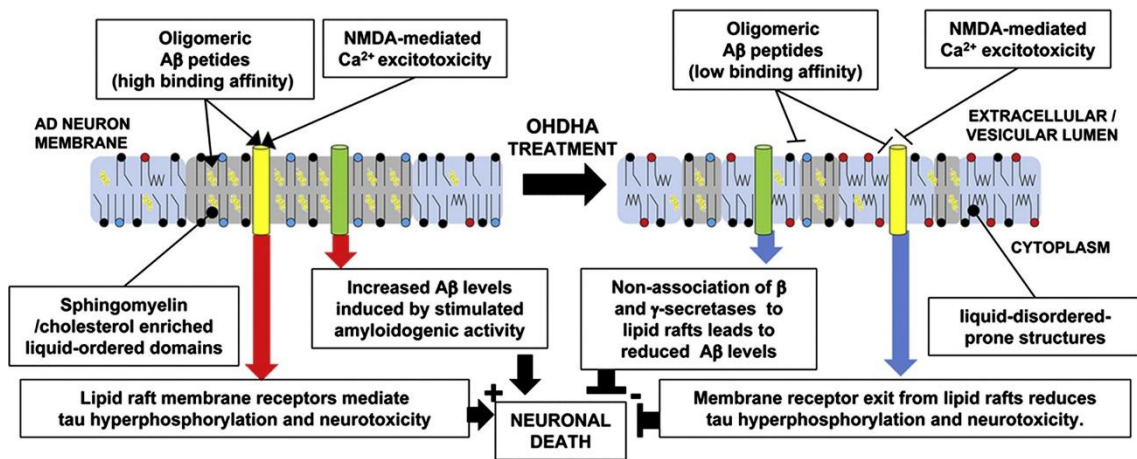
Figure S2
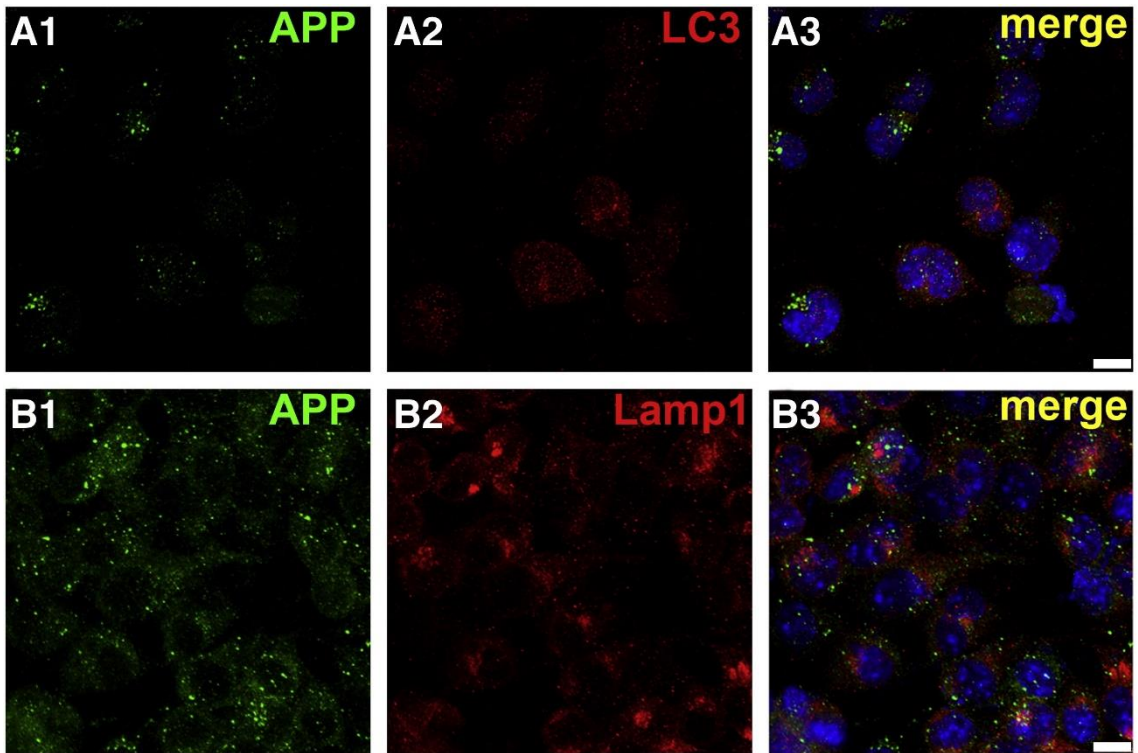
Figure S3

Figure S4

Graphical abstract

Highlights

- OHDHA increases the level of PE carrying DHA and other polyunsaturated fatty acids.
- OHDHA reduces Aβ levels and Aβ-induced tau phosphorylation.
- OHDHA protects neuron-like cells against oligomeric-Aβ and NMDA/Ca^{2+}-induced toxicity.
- OHDHA reduces affinity of fibrillar/oligomeric Aβ for lipid-raft membranes.
- OHDHA showed no remarkable toxicity at therapeutic doses.